Imaging junctions of waveguides

Laurent Bourgeois, Jean-François Fritsch, Arnaud Recoquillay

Imaging junctions of waveguides

April 30, 2020

Laurent Bourgeois

Laboratoire POEMS, ENSTA Paris,
828 Boulevard des Maréchaux, 91120 Palaiseau, France

Jean-François Fritsch

Laboratoire POEMS, ENSTA Paris,
828 Boulevard des Maréchaux, 91120 Palaiseau, France
and
CEA, LIST
91191 Gif-sur-Yvette, France

Arnaud Recoquillay

CEA, LIST
91191 Gif-sur-Yvette, France

Abstract

In this paper we address the identification of defects by the Linear Sampling Method in half-waveguides which are related to each other by junctions. Firstly a waveguide which is characterized by an abrupt change of properties is considered, secondly the more difficult case of several half-waveguides related to each other by a junction of complex geometry. Our approach is illustrated by some two-dimensional numerical experiments.

1 Introduction

This article deals with the identification of defects in junctions of waveguides. It is well-known that defects such as cracks often occur in weld bead of metallic pipes, which can be seen as junctions of waveguides. This explains why it is necessary to adapt Non Destructive Testing procedures to that kind of configuration. Assume that several emitters produce incident waves and that several receivers measure the corresponding scattered waves. The obtained set of data is called multistatic data, which contains a lot of information on the defects. The method that we wish to use in order to exploit this information is the Linear Sampling Method, which was first introduced in [1] and has proved its efficiency in many situations since that time (see for example [2]). The Linear Sampling Method consists in testing if some point z of a sampling grid is such that an analytically known test function depending on z belongs to the range of an integral operator, the kernel of which

exactly consists of our multistatic data. If it is the case, this means that z does belong to the defects. By testing all the points z of the grid, the LSM hence provides the indicator function of the defects, in other words an image of the defects. The LSM has a very interesting feature: its formulation does not depend on the number and nature of the defects. In practice, one has to solve, for each point z, a small system called the near-field equation. Such near-field equation is ill-posed and hence has to be regularized. In [3], the authors introduced a modal formulation of the LSM in the case of homogeneous waveguides. Such formulation takes advantage of the specific geometry of the waveguide to propose a physical way of regularizing the problem. It consists in decomposing both the incident and the scattered waves on the guided modes, which are either propagating or evanescent, and in considering the sole propagating modes in the inversion, the evanescent ones being neglected. Such clear decomposition is specific to waveguides. This procedure was used in many kinds of waveguides in the frequency domain, for example elastic waveguides [4, 5] or periodic waveguides [6]. A multi-frequency extension of the modal formulation of the Linear Sampling Method was done in [7], as an alternative choice to the full-time domain LSM used in [8]. Note that in [9], our method was successfully tested in the presence of real data coming from an ultrasonic NDT experiment on a steel plate. We here mention several other works based on sampling-type methods in acoustic waveguides [10, 11, 12, 13, 14, 15] and electromagnetic waveguides [16, 17].

The modal formulation in the case of homogeneous waveguides is easy to derive because the fundamental solution, which can be seen as a particular incident wave, has a simple expression in terms of the guided modes. This feature does not hold any more for the fundamental solution of a domain consisting of several half-waveguides linked to each other by a junction, that is why such a domain requires a specific treatment and justifies the present article. The main ingredients which enable us to apply the Linear Sampling Method for that complex geometry are the so-called reference fields, which are the scattering responses of the guided modes due to the sole junction in the absence of defects, and the reciprocity property satisfied by the fundamental solution in the whole domain, in the absence of the defects as well. These two ingredients allow us to easily compute the test function for all sampling point z, in the sense that such computation does not require a Finite Element computation for each z.

Having in mind the complicated problem of a junction of several waveguides, in this article we proceed step by step and propose the following organization. In section 2, we introduce the case of a waveguide characterized by an abrupt change of properties, more precisely a jump of the refractive index and of the transverse section. In section 3, we add a junction of complex geometry between our two half-waveguides. We extend this situation to the quite general case of a junction of complex geometry between several half-waveguides in section 4. Section 5 is dedicated to some numerical experiments in $2D$ which illustrate the feasibility of imaging junctions of waveguides. Section 6 consists of a short conclusion presenting possible extensions.

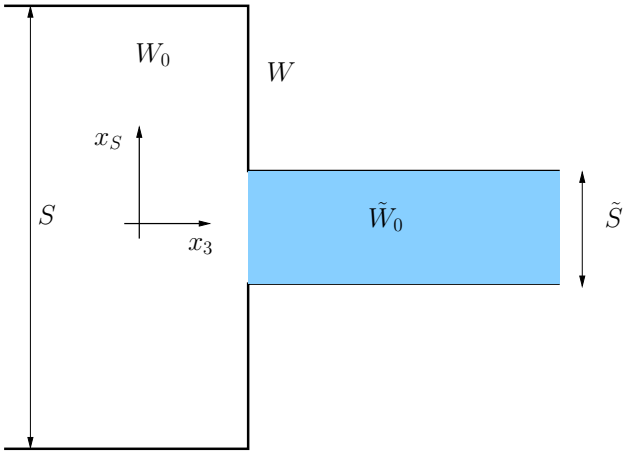

Figure 1: Waveguide with an abrupt change of properties

2 A waveguide with an abrupt change of properties

2.1 The guided modes

Let us consider the union W of two half-waveguides which have the same unbounded direction and which are in contact, the first one (the left one) of generic transverse section S, the second one (the right one) of generic transverse section $\tilde{S}$, with $S \cap \tilde{S} \neq \varnothing$. In order to simplify the presentation, we assume that either $S \subset \tilde{S}$ or $\tilde{S} \subset S$. Here, S is either an interval of $\mathbb{R}$ or a smooth connected bounded domain of $\mathbb{R}^2$, so that W is either a 2D or a 3D waveguide. Let us introduce the transverse sections $\Sigma_0 = S \times \{0\}$ and $\tilde{\Sigma}_0 = \tilde{S} \times \{0\}$, which separate the waveguide W into the left half-waveguide $W_0 = S \times (-\infty, 0)$ and the right half-waveguide $\tilde{W}_0 = \tilde{S} \times (0, +\infty)$. We also denote by $\mathcal{W}$ (resp. $\tilde{\mathcal{W}}$) the straight waveguide of section S (resp. $\tilde{S}$). We denote (x_S, x_3) the coordinates of a generic point x of W, where x_S is the coordinate in the transverse section S and x_3 is the coordinate along the unbounded direction of the waveguide. The acoustic field u in the waveguide W satisfies the standard Helmholtz equation

$$\Delta u + k^2 \eta^2 u = 0,$$

where k is the wave number and η is the refractive index, which is piecewise constant, namely there exists a constant $\tilde{n} > 0$ such that

$$\eta(x) = \begin{cases} 1 & \text{if} \quad x \in W_0 \\ \tilde{n} & \text{if} \quad x \in \tilde{W}_0. \end{cases} \tag{1}$$

In what follows, we will denote $\kappa = k$ and $\tilde{\kappa} = \tilde{n}k$. Our waveguide W is then characterized by an abrupt change of material and transverse section at $x_3 = 0$ (see Figure 1). Let us introduce the solutions of the Neumann eigenvalue problem for

the transverse Laplacian $\Delta_\perp$ in S, that is

$$\begin{cases} -\Delta_\perp \theta = \lambda\, \theta & \text{in} \quad S \\ \partial_{\nu_\perp} \theta = 0 & \text{on} \quad \partial S, \end{cases} \tag{2}$$

where $\nu_\perp$ is the outward normal on ∂S. It is well-known that the eigenvalues λ_n, $n \in \mathbb{N}$, form an increasing sequence of positive reals such that $\lambda_n \to +\infty$, while the corresponding eigenfunctions θ_n, $n \in \mathbb{N}$, may be chosen such that they form a complete orthonormal basis of $L^2(S)$. By replacing the section S by $\tilde{S}$, we similarly define the eigenvalues and eigenfunctions $(\tilde{\lambda}_n, \tilde{\theta}_n)$, $n \in \mathbb{N}$. Let us set, for all $n \in \mathbb{N}$,

$$\beta_n = \begin{cases} \sqrt{\kappa^2 - \lambda_n} & \text{if} \quad \kappa^2 - \lambda_n \geqslant 0 \\ i\sqrt{\lambda_n - \kappa^2} & \text{if} \quad \kappa^2 - \lambda_n < 0 \end{cases} \tag{3}$$

and let us define the $\tilde{\beta}_n$ similarly with κ replaced by $\tilde{\kappa}$ and λ_n replaced by $\tilde{\lambda}_n$. We assume that none of the β_n and none of the $\tilde{\beta}_n$ do vanish. Let us denote P (resp. $\tilde{P}$) in $\mathbb{N}$ such that for $n = 0, \ldots, P-1$ (resp. $n = 0, \ldots, \tilde{P}-1$) the number β_n (resp. $\tilde{\beta}_n$) is purely real. Let us introduce the solutions u and $\tilde{u}$ to the problems

$$\begin{cases} \Delta u + \kappa^2 u = 0 & \text{in} \quad \mathcal{W} \\ \partial_\nu u = 0 & \text{on} \quad \partial\mathcal{W}, \end{cases} \qquad \begin{cases} \Delta \tilde{u} + \tilde{\kappa}^2 \tilde{u} = 0 & \text{in} \quad \tilde{\mathcal{W}} \\ \partial_\nu \tilde{u} = 0 & \text{on} \quad \partial\tilde{\mathcal{W}}, \end{cases} \tag{4}$$

which in addition are products of a function of x_S and of a function of x_3. Here, ν is the outward normal on $\partial\mathcal{W}$ or $\partial\tilde{\mathcal{W}}$. It is easy to check that these solutions are given, for $n \in \mathbb{N}$, by

$$\begin{cases} g_n^\pm(x) = e^{\pm i\beta_n x_3} \theta_n(x_S) & \text{for} \quad x = (x_S, x_3) \in \mathcal{W} \\ \tilde{g}_n^\pm(x) = e^{\pm i\tilde{\beta}_n x_3} \tilde{\theta}_n(x_S) & \text{for} \quad x = (x_S, x_3) \in \tilde{\mathcal{W}}, \end{cases}$$

respectively, and are referred to as the guided modes in $\mathcal{W}$ and $\tilde{\mathcal{W}}$ in what follows. It is important to note that for $n = 0, \ldots, P-1$, the guided mode g_n^+ (resp. g_n^-) is propagating from the left to the right (resp. the right to the left), while for $n = P, \ldots, +\infty$, the guided mode g_n^+ (resp. g_n^-) is evanescent from the left to the right (resp. the right to the left). The same remark applies to the $\tilde{g}_n^\pm$.

2.2 The reference fields

We now need to introduce the so-called reference fields u_n and $\tilde{u}_n$ for all $n \in \mathbb{N}$. Let us denote $g_{n,0}^+$ the extension of g_n^+ in W_0 by 0 in $\tilde{W}_0$ and $\tilde{g}_{n,0}^-$ the extension of $\tilde{g}_n^-$ in $\tilde{W}_0$ by 0 in W_0, that is

$$g_{n,0}^+(x) = \begin{cases} g_n^+(x) & \text{if} \quad x \in W_0 \\ 0 & \text{if} \quad x \in \tilde{W}_0 \end{cases} \quad \text{and} \quad \tilde{g}_{n,0}^-(x) = \begin{cases} 0 & \text{if} \quad x \in W_0 \\ \tilde{g}_n^-(x) & \text{if} \quad x \in \tilde{W}_0. \end{cases}$$

We consider the following problems: find u_n and $\tilde{u}_n$ in $H^1_{\text{loc}}(W)$ such that

$$\begin{cases} \Delta u_n + k^2 \eta^2 u_n = 0 & \text{in} \quad W \\ \partial_\nu u_n = 0 & \text{on} \quad \partial W \\ u_n - g_{n,0}^+ & \text{is outgoing} \end{cases} \tag{5}$$

and

$$\begin{cases} \Delta\tilde{u}_n + k^2\eta^2\tilde{u}_n = 0 & \text{in} \qquad W \\ \partial_\nu \tilde{u}_n = 0 & \text{on} \qquad \partial W \\ \tilde{u}_n - \tilde{g}^-_{n,0} & \text{is outgoing.} \end{cases} \tag{6}$$

In problems (5) and (6), the fields u_n and $\tilde{u}_n$ can be viewed as total fields, the fields $g^+_{n,0}$ and $\tilde{g}^-_{n,0}$ as incident fields, while the fields $u_n - g^+_{n,0}$ and $\tilde{u}_n - \tilde{g}^-_{n,0}$ are scattered fields. The last line of the two systems (5) and (6) is a radiation condition which applies to the scattered fields. We say that the scattered field w is outgoing if there exist two sequences $(a_m)_{m\in\mathbb{N}}$ and $(b_m)_{m\in\mathbb{N}}$ of complex numbers and some $R > 0$ such that

$$\begin{cases} w(x) = \displaystyle\sum_{m\in\mathbb{N}} a_m\, e^{-i\beta_m x_3}\theta_m(x_S) & \text{for} \quad x = (x_S, x_3) \in W_0, \qquad x_3 < -R \\ w(x) = \displaystyle\sum_{m\in\mathbb{N}} b_m\, e^{i\tilde{\beta}_m x_3}\tilde{\theta}_m(x_S) & \text{for} \quad x = (x_S, x_3) \in \tilde{W}_0, \qquad x_3 > R. \end{cases} \tag{7}$$

Let us define the Dirichlet-To-Neumann maps T on $\Sigma_{-R} = S \times \{-R\}$ and $\tilde{T}$ on $\tilde{\Sigma}_R = \tilde{S} \times \{R\}$, with

$$\begin{cases} T : H^{1/2}(\Sigma_{-R}) \to \tilde{H}^{-1/2}(\Sigma_{-R}) \\ \quad h \mapsto Th = \displaystyle\sum_{m\in\mathbb{N}} i\beta_m (h, \theta_m)_{L^2(S)}\theta_m \end{cases} \tag{8}$$

and

$$\begin{cases} \tilde{T} : H^{1/2}(\tilde{\Sigma}_R) \to \tilde{H}^{-1/2}(\tilde{\Sigma}_R) \\ \quad \tilde{h} \mapsto \tilde{T}\tilde{h} = \displaystyle\sum_{m\in\mathbb{N}} i\tilde{\beta}_m (\tilde{h}, \tilde{\theta}_m)_{L^2(\tilde{S})}\tilde{\theta}_m, \end{cases} \tag{9}$$

where $\tilde{H}^{-1/2}(\Sigma_{-R})$ denotes the dual space of $H^{1/2}(\Sigma_{-R})$ and $\tilde{H}^{-1/2}(\tilde{\Sigma}_R)$ the dual space of $H^{1/2}(\tilde{\Sigma}_R)$. We recall here that if S is a bounded domain of $\mathbb{R}^d$ $(d = 1, 2)$, $H^{1/2}(S)$ is the set of restrictions on S of functions in $H^{1/2}(\mathbb{R}^d)$, while $\tilde{H}^{-1/2}(S)$ coincides with the set of distributions in $H^{-1/2}(\mathbb{R}^d)$ which are supported in $\overline{S}$. It is well-known that the radiation condition (7) is equivalent to

$$-\partial_{x_3} w|_{\Sigma_{-R}} = T(w|_{\Sigma_{-R}}) \quad \text{and} \quad \partial_{x_3} w|_{\tilde{\Sigma}_R} = \tilde{T}(w|_{\tilde{\Sigma}_R}). \tag{10}$$

Let us denote W^b_R the bounded domain W between the sections Σ_{-R} and $\tilde{\Sigma}_R$, Γ^b_R the boundary of ∂W between the sections Σ_{-R} and $\tilde{\Sigma}_R$.

Proposition 1. *For all $n \in \mathbb{N}$, the systems (5) and (6) have both a unique solution in $H^1_{\text{loc}}(W)$.*

Proof. We only address system (5), the second one would be treated similarly. Problem (5) is equivalent to: find $u_n \in H^1(W^b_R)$ such that

$$\begin{cases} \Delta u_n + k^2\eta^2 u_n = 0 & \text{in} \quad W^b_R \\ \partial_\nu u_n = 0 & \text{on} \quad \Gamma^b_R \\ -\partial_{x_3} u_n = Tu_n - 2i\beta_n g^+_n & \text{on} \quad \Sigma_{-R} \\ \partial_{x_3} u_n = \tilde{T}u_n & \text{on} \quad \tilde{\Sigma}_R. \end{cases} \tag{11}$$

Here, we have used the fact that $g^+_{n,0} = g^+_n$ on Σ_{-R}, that $g^+_{n,0} = 0$ on $\tilde{\Sigma}_R$ and

$$\partial_{x_3} g^+_n|_{\Sigma_{-R}} + T(g^+_n|_{\Sigma_{-R}}) = 2i\beta_n g^+_n|_{\Sigma_{-R}}.$$

An equivalent weak formulation to (11) is: find $u_n \in H^1(W^b_R)$ such that for all $v \in H^1(W^b_R)$,

$$a(u_n, v) = \ell(v), \tag{12}$$

where

$$a(u,v) = \int_{W^b_R} (\nabla u \cdot \nabla \overline{v} - k^2\eta^2 u\overline{v})\, dx - \int_{\Sigma_{-R}} Tu\overline{v}\, ds - \int_{\tilde{\Sigma}_R} \tilde{T}u\overline{v}\, ds \tag{13}$$

and

$$\ell(v) = -\int_{\Sigma_{-R}} 2i\beta_n g^+_n \overline{v}\, ds. \tag{14}$$

Here the integrals on the transverse sections have the meaning of duality pairing between $\tilde{H}^{-1/2}(\Sigma_{-R})$ and $H^{1/2}(\Sigma_{-R})$ or between $\tilde{H}^{-1/2}(\tilde{\Sigma}_R)$ and $H^{1/2}(\tilde{\Sigma}_R)$. By introducing the sesquilinear forms b and c such that $a = b + c$, with b and c defined by

$$b(u,v) = \int_{W^b_R} (\nabla u \cdot \nabla \overline{v} + u\overline{v})\, dx - \int_{\Sigma_{-R}} Tu\overline{v}\, ds - \int_{\tilde{\Sigma}_R} \tilde{T}u\overline{v}\, ds,$$

$$c(u,v) = -\int_{W^b_R} (1 + k^2\eta^2) u\overline{v}\, dx,$$

we notice that

$$\begin{aligned}
\mathrm{Re}\,\{b(u,u)\} &= \int_{W^b_R} (|\nabla u|^2 + |u|^2)\, dx \\
&\quad + \sum_{n=P}^{+\infty} \sqrt{\lambda_n - \kappa^2}\, \left|(u, \theta_n)_{L^2(S)}\right|^2 + \sum_{n=\tilde{P}}^{+\infty} \sqrt{\tilde{\lambda}_n - \tilde{\kappa}^2}\, \left|(u, \tilde{\theta}_n)_{L^2(\tilde{S})}\right|^2 \\
&\geqslant \|u\|^2_{H^1(W^b_R)}.
\end{aligned}$$

This implies that the weak problem (12) is of Fredholm type, hence uniqueness implies existence. It remains to prove uniqueness. Let us assume that two functions in $H^1_{\mathrm{loc}}(W)$ satisfy problems (5). The difference w between these two functions then simultaneously satisfies the two problems (4) in W_0 and $\tilde{W}_0$, respectively. By projecting w on the basis (θ_n) in W_0 and on the basis $(\tilde{\theta}_n)$ in $\tilde{W}_0$, we obtain that

$$\begin{cases} w(x) = \displaystyle\sum_{n\in\mathbb{N}} \left(c_n g^+_n(x) + a_n g^-_n(x)\right) =: w_-(x), & x \in W_0 \\ w(x) = \displaystyle\sum_{n\in\mathbb{N}} \left(b_n \tilde{g}^+_n(x) + d_n \tilde{g}^-_n(x)\right) =: w_+(x), & x \in \tilde{W}_0. \end{cases}$$

Since w satisfies the radiation condition, we have $c_n = 0$ and $d_n = 0$ for all $n \in \mathbb{N}$, so that

$$w_-(x_S, x_3) = \sum_{n\in\mathbb{N}} a_n e^{-i\beta_n x_3} \theta_n(x_S), \quad w_+(x_S, x_3) = \sum_{n\in\mathbb{N}} b_n e^{i\tilde{\beta}_n x_3} \tilde{\theta}_n(x_S). \tag{15}$$

Without loss of generality, we assume that $\tilde{S} \subset S$ (as in the figure 1). Let us denote $h = w_-|_{\Sigma_0} \in H^{1/2}(\Sigma_0)$, then $a_n = (h, \theta_n)_{L^2(S)}$ for all $n \in \mathbb{N}$. By continuity of the trace on $\tilde{\Sigma}_0 \subset \Sigma_0$, we have $h|_{\tilde{\Sigma}_0} = w_+|_{\tilde{\Sigma}_0}$, hence $b_n = (h|_{\tilde{S}}, \tilde{\theta}_n)_{L^2(\tilde{S})}$ for all $n \in \mathbb{N}$. Since $\partial_{x_3} w_- = 0$ on $\Sigma_0 \backslash \tilde{\Sigma}_0$, we have $\partial_{x_3} w_-|_{\Sigma_0} \in \tilde{H}^{-1/2}(\Sigma_0)$ and denoting $E(\partial_{x_3} w_+|_{\tilde{\Sigma}_0})$ the extension of $\partial_{x_3} w_+|_{\tilde{\Sigma}_0}$ on Σ_0 by 0, we have $E(\partial_{x_3} w_+|_{\tilde{\Sigma}_0}) \in \tilde{H}^{-1/2}(\Sigma_0)$ and

$$\partial_{x_3} w_-|_{\Sigma_0} = E(\partial_{x_3} w_+|_{\tilde{\Sigma}_0})$$

on Σ_0, which implies in particular

$$\begin{aligned} \langle \partial_{x_3} w_-|_{\Sigma_0}, h \rangle_{\tilde{H}^{-1/2}(\Sigma_0), H^{1/2}(\Sigma_0)} &= \langle E(\partial_{x_3} w_+|_{\tilde{\Sigma}_0}), h \rangle_{\tilde{H}^{-1/2}(\Sigma_0), H^{1/2}(\Sigma_0)} \\ &= \langle \partial_{x_3} w_+|_{\tilde{\Sigma}_0}, h|_{\tilde{\Sigma}_0} \rangle_{\tilde{H}^{-1/2}(\tilde{\Sigma}_0), H^{1/2}(\tilde{\Sigma}_0)}, \end{aligned}$$

that is, from (15),

$$\sum_{n \in \mathbb{N}} (-i\beta_n) a_n (\theta_n, h)_{L^2(S)} = \sum_{n \in \mathbb{N}} (i\tilde{\beta}_n) b_n (\tilde{\theta}_n, h|_{\tilde{S}})_{L^2(\tilde{S})},$$

and lastly

$$\sum_{n \in \mathbb{N}} \beta_n \left| (h, \theta_n)_{L^2(S)} \right|^2 + \sum_{n \in \mathbb{N}} \tilde{\beta}_n |(h|_{\tilde{S}}, \tilde{\theta}_n)_{L^2(\tilde{S})}|^2 = 0.$$

Decomposing the first sum into $\sum_{n=0}^{P-1}$ and $\sum_{n=P}^{+\infty}$ and the second one into $\sum_{n=0}^{\tilde{P}-1}$ and $\sum_{n=\tilde{P}}^{+\infty}$, taking the real and the imaginary parts, yields $a_n = (h, \theta_n)_{L^2(S)} = 0$ and $b_n = (h|_{\tilde{S}}, \tilde{\theta}_n)_{L^2(\tilde{S})} = 0$ for all $n \in \mathbb{N}$. Then $w = 0$ in W, which completes the proof. □

Taking inspiration from the mode matching method described in [18], instead of the weak formulation (12) for u_n in $H^1(W_R^b)$ we can also derive a weak formulation for the trace $\varphi_n := u_n|_{\Sigma_0}$ in $H^{1/2}(S)$.

Proposition 2. *Assume that $\tilde{S} \subset S$. The function φ_n is the unique solution to the weak formulation: find $\varphi_n \in H^{1/2}(S)$ such that for all $\psi \in H^{1/2}(S)$,*

$$\begin{cases} \displaystyle\sum_{m \in \mathbb{N}} \beta_m (\varphi_n, \theta_m)_{L^2(S)} \overline{(\psi, \theta_m)_{L^2(S)}} + \sum_{m \in \mathbb{N}} \tilde{\beta}_m (\varphi_n|_{\tilde{S}}, \tilde{\theta}_m)_{L^2(\tilde{S})} \overline{(\psi|_{\tilde{S}}, \tilde{\theta}_m)_{L^2(\tilde{S})}} \\ \qquad\qquad = 2\beta_n \overline{(\psi, \theta_n)_{L^2(S)}}. \end{cases}$$

Proof. Indeed, there exist two sequences of complex numbers $(a_m)_{m \in \mathbb{N}}$ and $(b_m)_{m \in \mathbb{N}}$ such that

$$\begin{cases} u_{n-}(x) = \quad g_n^+(x) + \displaystyle\sum_{m \in \mathbb{N}} a_m g_m^-(x), \quad x \in W_0 \\ u_{n+}(x) = \displaystyle\sum_{m \in \mathbb{N}} b_m \tilde{g}_m^+(x), \quad x \in \tilde{W}_0. \end{cases}$$

Using that $\varphi_n = u_n|_{\Sigma_0}$, we obtain that $a_m = (\varphi_n, \theta_m)_{L^2(S)} - \delta_{mn}$ for all $m \in \mathbb{N}$. Similarly, we have $b_m = (\varphi_n|_{\tilde{S}}, \tilde{\theta}_m)_{L^2(\tilde{S})}$ for all $m \in \mathbb{N}$. Hence

$$\begin{cases} \partial_{x_3} u_{n-}|_{\Sigma_0} = \quad 2i\beta_n \theta_n - \displaystyle\sum_{m \in \mathbb{N}} i\beta_m (\varphi_n, \theta_m)_{L^2(S)} \theta_m, \\ \partial_{x_3} u_{n+}|_{\tilde{\Sigma}_0} = \displaystyle\sum_{m \in \mathbb{N}} i\tilde{\beta}_m (\varphi_n|_{\tilde{S}}, \tilde{\theta}_m)_{L^2(\tilde{S})} \tilde{\theta}_m. \end{cases} \tag{16}$$

That

$$\partial_{x_3} u_{n-}|_{\Sigma_0} = E(\partial_{x_3} u_{n+}|_{\tilde{\Sigma}_0})$$

in the space $\tilde{H}^{-1/2}(\Sigma_0)$ implies that for all $\psi \in H^{1/2}(\Sigma_0)$,

$$\langle \partial_{x_3} u_{n-}|_{\Sigma_0}, \psi \rangle = \langle \partial_{x_3} u_{n+}|_{\tilde{\Sigma}_0}, \psi|_{\tilde{\Sigma}_0} \rangle,$$

which yields the weak formulation of Proposition 2 in view of (16). It is easy to prove that such weak formulation is well-posed by the Lax-Milgram lemma. □

2.3 The fundamental solution

Let us now introduce the fundamental solution of the waveguide W. For $y \in W$, we consider the problem: find $G(\cdot, y) \in L^2_{\rm loc}(W)$ such that

$$\begin{cases} -(\Delta G(\cdot, y) + k^2 \eta^2 G(\cdot, y)) = \delta_y & \text{in} \quad W \\ \partial_\nu G(\cdot, y) = 0 & \text{on} \quad \partial W \\ G(\cdot, y) & \text{is outgoing.} \end{cases} \tag{17}$$

For $y \in \mathcal{W}$ (resp. $\tilde{\mathcal{W}}$), let us denote by $\mathcal{G}(\cdot, y)$ (resp. $\tilde{\mathcal{G}}(\cdot, y)$) the fundamental solution of the straight and homogeneous waveguide $\mathcal{W}$ (resp. $\tilde{\mathcal{W}}$) with wave number κ (resp. $\tilde{\kappa}$). It is well-known that $\mathcal{G}(\cdot, y)$ and $\tilde{\mathcal{G}}(\cdot, y)$ are given by

$$\mathcal{G}(x, y) = -\sum_{n \in \mathbb{N}} \frac{1}{2i\beta_n} e^{i\beta_n |x_3 - y_3|} \theta_n(x_S) \theta_n(y_S), \quad (x, y) \in \mathcal{W} \times \mathcal{W},$$

$$\tilde{\mathcal{G}}(x, y) = -\sum_{n \in \mathbb{N}} \frac{1}{2i\tilde{\beta}_n} e^{i\tilde{\beta}_n |x_3 - y_3|} \tilde{\theta}_n(x_S) \tilde{\theta}_n(y_S), \quad (x, y) \in \tilde{\mathcal{W}} \times \tilde{\mathcal{W}}.$$

For $y \in W_0$ (resp. in $\tilde{W}_0$), we also denote $\mathcal{G}_0(\cdot, y)$ (resp. $\tilde{\mathcal{G}}_0(\cdot, y)$) the fields defined by

$$\mathcal{G}_0(x, y) = \begin{cases} \mathcal{G}(x, y) & \text{if} \quad x \in W_0 \\ 0 & \text{if} \quad x \in \tilde{W}_0 \end{cases} \quad \text{and} \quad \tilde{\mathcal{G}}_0(x, y) = \begin{cases} 0 & \text{if} \quad x \in W_0 \\ \tilde{\mathcal{G}}(x, y) & \text{if} \quad x \in \tilde{W}_0. \end{cases}$$

We have the following result.

Proposition 3. *The problem (17) has a unique solution in $L^2_{\rm loc}(W)$ which is given by the following formulas:*

- *for $y \in W_0$ and $x \in W$,*

$$G(x, y) = \begin{cases} \mathcal{G}(x, y) - \displaystyle\sum_{n \in \mathbb{N}} \frac{1}{2i\beta_n} g_n^-(y)(u_n(x) - g_n^+(x)) & \text{for} \quad x_3 < y_3 \\ \qquad\qquad - \displaystyle\sum_{n \in \mathbb{N}} \frac{1}{2i\beta_n} g_n^-(y) u_n(x) & \text{for} \quad x_3 > y_3, \end{cases} \tag{18}$$

- *for $y \in \tilde{W}_0$ and $x \in W$,*

$$G(x, y) = \begin{cases} \qquad - \displaystyle\sum_{n \in \mathbb{N}} \frac{1}{2i\tilde{\beta}_n} \tilde{g}_n^+(y) \tilde{u}_n(x) & \text{for} \quad x_3 < y_3 \\ \tilde{\mathcal{G}}(x, y) - \displaystyle\sum_{n \in \mathbb{N}} \frac{1}{2i\tilde{\beta}_n} \tilde{g}_n^+(y)(\tilde{u}_n(x) - \tilde{g}_n^-(x)) & \text{for} \quad x_3 > y_3, \end{cases}$$

where u_n and $\tilde{u}_n$ are the solutions to problems (5) and (6), respectively.

Proof. We only consider the case when $y \in W_0$, that is we prove (18) (the case $y \in \tilde{W}_0$ is similar). Without loss of generality, we assume that $\tilde{S} \subset S$. We use the decomposition $G(\cdot, y) = \mathcal{G}_0(\cdot, y) + \mathcal{G}^s(\cdot, y)$, where $\mathcal{G}_0(\cdot, y)$ plays the role of an incident wave while $\mathcal{G}^s(\cdot, y)$ plays the role of a scattered wave. The field $\mathcal{G}^s(\cdot, y)$ satisfies the transmission problem

$$\begin{cases} \Delta \mathcal{G}^s(\cdot, y) + k^2 \eta^2 \mathcal{G}^s(\cdot, y) = 0 & \text{in} \quad W_0 \cup \tilde{W}_0 \\ \partial_\nu \mathcal{G}^s(\cdot, y) = 0 & \text{on} \quad \partial W \\ [\![\mathcal{G}^s(\cdot, y)]\!] = \mathcal{G}(\cdot, y) & \text{on} \quad \tilde{\Sigma}_0 \\ [\![\partial_{x_3} \mathcal{G}^s(\cdot, y)]\!] = \partial_{x_3} \mathcal{G}(\cdot, y) & \text{on} \quad \Sigma_0 \\ \mathcal{G}^s(\cdot, y) & \text{is outgoing.} \end{cases} \tag{19}$$

Here, the notation $[\![\cdot]\!]$ means the jump from the left to the right. The values of $\partial_{x_3} \mathcal{G}^s(\cdot, y)$ and $\partial_{x_3} \mathcal{G}_0(\cdot, y)$, which have no meaning on $\Sigma_0 \backslash \tilde{\Sigma}_0$ from the right, are arbitrarily fixed to 0. With this convention, the transmission conditions hold in $H^{1/2}(\tilde{\Sigma}_0)$ and $\tilde{H}^{-1/2}(\Sigma_0)$, respectively. By using a similar weak formulation as in Proposition 1 in the bounded domain W_R^b, we would prove that problem (19) has a unique solution $\mathcal{G}^s(\cdot, y)$ such that $(\mathcal{G}^s(\cdot, y)|_{W_0}, \mathcal{G}^s(\cdot, y)|_{\tilde{W}_0}) \in H^1_{\text{loc}}(W_0) \times H^1_{\text{loc}}(\tilde{W}_0)$. Then $G(\cdot, y) = \mathcal{G}_0(\cdot, y) + \mathcal{G}^s(\cdot, y)$ is the solution to problem (17). Next, we remark by using the decomposition $u_n = g^+_{n,0} + v^s_n$ for all $n \in \mathbb{N}$, where $g^+_{n,0}$ plays the role of an incident wave while v^s_n plays the role of a scattered wave, that the field v^s_n satisfies the transmission problem

$$\begin{cases} \Delta v^s_n + k^2 \eta^2 v^s_n = 0 & \text{in} \quad W_0 \cup \tilde{W}_0 \\ \partial_\nu v^s_n = 0 & \text{on} \quad \partial W \\ [\![v^s_n]\!] = g^+_n & \text{on} \quad \tilde{\Sigma}_0 \\ [\![\partial_{x_3} v^s_n]\!] = \partial_{x_3} g^+_n & \text{on} \quad \Sigma_0 \\ v^s_n(\cdot, y) & \text{is outgoing,} \end{cases} \tag{20}$$

with the same convention as above concerning the values of $\partial_{x_3} v^s_n$ and $\partial_{x_3} g^+_{n,0}$ from the right on $\Sigma_0 \backslash \tilde{\Sigma}_0$. Since $y_3 < 0$, for $x_3 = 0$ we have

$$\begin{aligned} \mathcal{G}(x, y) &= -\sum_{n \in \mathbb{N}} \frac{1}{2i\beta_n} e^{i\beta_n (x_3 - y_3)} \theta_n(x_S) \theta_n(y_S) \\ &= -\sum_{n \in \mathbb{N}} \frac{1}{2i\beta_n} g^-_n(y) g^+_n(x). \end{aligned}$$

Comparing systems (19) and (20), by linearity we obtain that for $y \in W_0$ and $x \in W$, we have

$$\mathcal{G}^s(x, y) = -\sum_{n \in \mathbb{N}} \frac{1}{2i\beta_n} g^-_n(y) v^s_n(x).$$

Formula (18) is then obtained considering that for $x \in W_0$ we have $G(x, y) = \mathcal{G}(x, y) + \mathcal{G}^s(x, y)$ and that for $x \in \tilde{W}_0$ we have $G(x, y) = \mathcal{G}^s(x, y)$. It remains to observe that for $y \in W_0$ and $x \in W_0$, in the particular case $x_3 > y_3$ we have the

simplification

$$\begin{aligned} G(x,y) &= \mathcal{G}(x,y) - \sum_{n\in\mathbb{N}} \frac{1}{2i\beta_n} g_n^-(y)(u_n(x) - g_n^+(x)) \\ &= -\sum_{n\in\mathbb{N}} \frac{1}{2i\beta_n} g_n^-(y) g_n^+(x) - \sum_{n\in\mathbb{N}} \frac{1}{2i\beta_n} g_n^-(y)(u_n(x) - g_n^+(x)) \\ &= -\sum_{n\in\mathbb{N}} \frac{1}{2i\beta_n} g_n^-(y) u_n(x), \end{aligned}$$

which completes the proof. □

2.4 The case of a waveguide of constant section

An important particular case is when the sections of the two half-waveguides do coincide, that is $S = \tilde{S}$, then the fields u_n and $\tilde{u}_n$ that solve the systems (5) and (6) have a closed-form expression.

Proposition 4. *If $S = \tilde{S}$, for all $n \in \mathbb{N}$, the solutions to the systems (5) and (6) are given by*

$$u_n(x) = \begin{cases} g_n^+(x) + \dfrac{\beta_n - \tilde{\beta}_n}{\beta_n + \tilde{\beta}_n} g_n^-(x) & \text{for} \quad x \in W_0 \\ \dfrac{2\beta_n}{\beta_n + \tilde{\beta}_n} \tilde{g}_n^+(x) & \text{for} \quad x \in \tilde{W}_0, \end{cases} \tag{21}$$

and

$$\tilde{u}_n(x) = \begin{cases} \dfrac{2\tilde{\beta}_n}{\tilde{\beta}_n + \beta_n} g_n^-(x) & \text{for} \quad x \in W_0 \\ \tilde{g}_n^-(x) + \dfrac{\tilde{\beta}_n - \beta_n}{\tilde{\beta}_n + \beta_n} \tilde{g}_n^+(x) & \text{for} \quad x \in \tilde{W}_0. \end{cases}$$

Proof. Let us consider the case of problem (5), the case of (6) would be addressed exactly the same way. Let u_n be given by the formula (21), it is straightforward that $u_n \in H^1_{\mathrm{loc}}(W_0)$ and $u_n \in H^1_{\mathrm{loc}}(\tilde{W}_0)$, as well as $\Delta u_n + \kappa^2 u_n = 0$ in W_0 and $\Delta u_n + \tilde{\kappa}^2 u_n = 0$ in $\tilde{W}_0$. In order to prove that $u_n \in H^1_{\mathrm{loc}}(W)$ and $\Delta u_n + k^2\eta^2 u_n = 0$ in W in the sense of distributions, it suffices to prove that the left and right traces $u_n|_{\Sigma_0^-}$ and $u_n|_{\Sigma_0^+}$ coincide, as well as the left and right normal derivatives $\partial_{x_3} u_n|_{\Sigma_0^-}$ and $\partial_{x_3} u_n|_{\Sigma_0^+}$. We have

$$u_n|_{\Sigma_0^-}(x_S) = \theta_n(x_S) + \frac{\beta_n - \tilde{\beta}_n}{\beta_n + \tilde{\beta}_n} \theta_n(x_S) = \frac{2\beta_n}{\beta_n + \tilde{\beta}_n} \theta_n(x_S) = u_n|_{\Sigma_0^+}(x_S),$$

and

$$\begin{aligned} \partial_{x_3} u_n|_{\Sigma_0^-}(x_S) &= (i\beta_n) \left(1 - \frac{\beta_n - \tilde{\beta}_n}{\beta_n + \tilde{\beta}_n}\right) \theta_n(x_S) \\ &= (i\tilde{\beta}_n) \frac{2\beta_n}{\beta_n + \tilde{\beta}_n} \theta_n(x_S) = \partial_{x_3} u_n|_{\Sigma_0^+}(x_S), \end{aligned}$$

which is the result. The boundary condition $\partial_\nu u_n = 0$ on ∂W is satisfied because it is satisfied by the guided modes. As concerns the radiation condition, it is

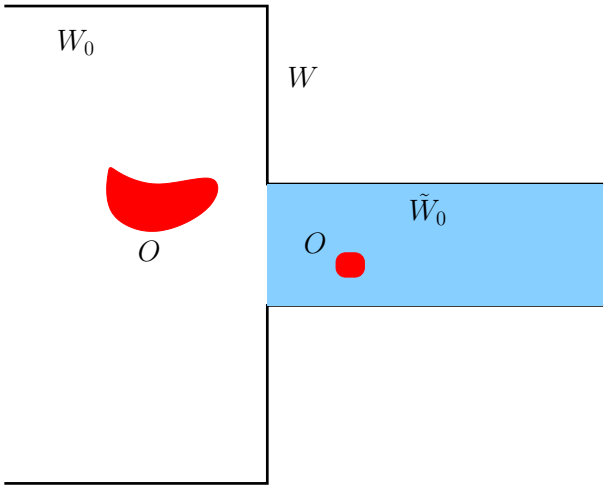

Figure 2: Obstacles within the waveguide

straightforward that $u_n - g^+_{n,0}$ is proportional to $g^-_n(x) = e^{-i\beta_n x_3}\theta_n(x_S)$ in W_0 and proportional to $\tilde{g}^+_n(x) = e^{i\tilde{\beta}_n x_3}\theta_n(x_S)$ in $\tilde{W}_0$, which completes the verification that u_n satisfies problem (5). Uniqueness in Proposition 1 completes the proof. □

Remark 1. From Proposition 4, it should be noted that for each incident guided mode, a single guided mode is reflected and a single guided mode is transmitted. In the expression (21) of the field u_n, for instance, the complex number $R_n = (\beta_n - \tilde{\beta}_n)/(\beta_n + \tilde{\beta}_n)$ is the reflection coefficient while the complex number $T_n = (2\beta_n)/(\beta_n + \tilde{\beta}_n)$ is the transmission coefficient related to the guided mode g^+_n.

It is important to note that if the sections of the two half-waveguides coincide then the fundamental solution in the waveguide W (that is the solution to problem (17)) has a closed-form expression, since the fields u_n and $\tilde{u}_n$ have a closed-form one (in view of Proposition 3 and Proposition 4).

2.5 The Linear Sampling Method

In this paragraph, we essentially adapt the results of [3] to the waveguide in the presence of an abrupt change of properties. In this view we introduce a generic forward scattering problem. We assume there exists an obstacle O within the waveguide W, more precisely O is a smooth and bounded open (not necessarily connected) domain such that $\overline{O} \subset W$, with $\Omega = W \backslash \overline{O}$ a connected open domain. For some $y \in \Omega$, let us consider the problem: find $u(\cdot, y) \in L^2_{\text{loc}}(\Omega)$ such that

$$\begin{cases} -(\Delta u(\cdot,y) + k^2\eta^2 u(\cdot,y)) = \delta_y & \text{in} \quad \Omega \\ \partial_\nu u(\cdot,y) = 0 & \text{on} \quad \partial W \\ u(\cdot,y) = 0 & \text{on} \quad \partial O \\ u(\cdot,y) & \text{is outgoing.} \end{cases} \tag{22}$$

By using the decomposition $u(\cdot,y) = G(\cdot,y) + u^s(\cdot,y)$, where $G(\cdot,y)$ is the solution to problem (17), the field $u(\cdot,y)$ can be viewed as a total field, the field $G(\cdot,y)$ as

an incident field and $u^s(\cdot, y)$ as a scattered field. Note that for some $y \in \Omega$, the scattered field $u^s(\cdot, y)$ satisfies the problem:

$$\begin{cases} \Delta u^s(\cdot, y) + k^2\eta^2 u^s(\cdot, y) = 0 & \text{in} \quad \Omega \\ \partial_\nu u^s(\cdot, y) = 0 & \text{on} \quad \partial W \\ u^s(\cdot, y) = f & \text{on} \quad \partial O \\ u^s(\cdot, y) & \text{is outgoing.} \end{cases} \tag{23}$$

with $f = -G(\cdot, y)|_{\partial O}$. We have the following proposition, the proof of which is very similar to the one of [19, Theorem 2.2].

Proposition 5. *For all $y \in \Omega$, the problem (23) has a unique solution in $H^1_{\text{loc}}(\Omega)$, except for at most a countable set of wave numbers k.*

The inverse problem is the following. We assume that we know $u^s(x, y)$ for all $(x, y) \in \hat{\Sigma}$ and want to retrieve O from those multistatic data. We consider either of the two following configurations concerning the amount of data, that is $\hat{\Sigma}$:

- $\hat{\Sigma} = \Sigma_{-R} \cup \tilde{\Sigma}_R$: full-scattering data
- $\hat{\Sigma} = \Sigma_{-R}$: back-scattering data,

where R is sufficiently large so that the obstacle O lies between the two transverse sections Σ_{-R} and $\tilde{\Sigma}_R$.

Remark 2. We note that for $y \in \Sigma_{-R}$, the identity $u^s(\cdot, y) = u(\cdot, y) - G(\cdot, y)$ can be rewritten

$$u^s(\cdot, y) = (u(\cdot, y) - \mathcal{G}_0(\cdot, y)) - (G(\cdot, y) - \mathcal{G}_0(\cdot, y)) .$$

Here, the field $u(\cdot, y) - \mathcal{G}_0(\cdot, y)$ represents the scattered field of the point source $\mathcal{G}_0(\cdot, y)$ due to the presence of both the abrupt change of properties between the two half-waveguides and the presence of the obstacle O, while the field $G(\cdot, y) - \mathcal{G}_0(\cdot, y)$ represents the scattered field of the same point source due to the change of properties only. In this sense, the data $u^s(x, y)$ for all $(x, y) \in \hat{\Sigma}$ can be viewed as differential measurements following the terminology introduced in [20].

Adapting the proof of [3, Theorem 1] we establish uniqueness for our inverse problems in both configurations, that is: if two obstacles are such that the corresponding multistatic data coincide, then they coincide. The Linear Sampling Method is an effective method which enables us to retrieve the obstacle O from the data $u^s(x, y)$, $(x, y) \in \hat{\Sigma}$, based on the near-field operator:

$$\begin{cases} N : L^2(\hat{\Sigma}) \to L^2(\hat{\Sigma}) \\ \quad \hat{h} \mapsto N\hat{h}, \quad (N\hat{h})(x) = \displaystyle\int_{\hat{\Sigma}} u^s(x, y)\hat{h}(y)\, ds(y), \quad x \in \hat{\Sigma}, \end{cases} \tag{24}$$

where $u^s(\cdot, y)$ is the solution to problem (23). We will also need the operator

$$\begin{cases} H : L^2(\hat{\Sigma}) \to H^{1/2}(\partial O) \\ \quad \hat{h} \mapsto (H\hat{h})(x) = \displaystyle\int_{\hat{\Sigma}} G(x, y)\hat{h}(y)\, ds(y), \quad x \in \partial O. \end{cases} \tag{25}$$

The Linear Sampling Method is justified by the following theorem, the proof of which mimics the one proved in [21].

Theorem 2.1. *We assume that the exterior problems (23) are well-posed and that the interior problem: find $w \in H^1(O)$ such that*

$$\begin{cases} \Delta w + k^2\eta^2 w = 0 & in \quad O \\ w = 0 & on \quad \partial O \end{cases}$$

has only the trivial solution. Let N and H be the operators defined by (24) and (25), respectively.

- *If $z \in O$, then for all $\varepsilon > 0$ there exists a solution $\hat{h}_\varepsilon(\cdot, z) \in L^2(\hat{\Sigma})$ of the inequality*

$$\|N\hat{h}_\varepsilon(\cdot, z) - G(\cdot, z)\|_{L^2(\hat{\Sigma})} \leqslant \varepsilon$$

  such that the function $H\hat{h}_\varepsilon(\cdot, z)$ converges in $H^{1/2}(\partial O)$ as $\varepsilon \to 0$. Furthermore, for a given fixed ε, the function $\hat{h}_\varepsilon(\cdot, z)$ satisfies

$$\lim_{z\to\partial O} \|\hat{h}_\varepsilon(\cdot, z)\|_{L^2(\hat{\Sigma})} = +\infty \quad and \quad \lim_{z\to\partial O} \|H\hat{h}_\varepsilon(\cdot, z)\|_{H^{1/2}(\partial O)} = +\infty.$$

- *If $z \in W\backslash\overline{O}$, then every solution $\hat{h}_\varepsilon(\cdot, z) \in L^2(\hat{\Sigma})$ of the inequality*

$$\|N\hat{h}_\varepsilon(\cdot, z) - G(\cdot, z)\|_{L^2(\hat{\Sigma})} \leqslant \varepsilon$$

  satisfies

$$\lim_{\varepsilon\to 0} \|\hat{h}_\varepsilon(\cdot, z)\|_{L^2(\hat{\Sigma})} = +\infty \quad and \quad \lim_{\varepsilon\to 0} \|H\hat{h}_\varepsilon(\cdot, z)\|_{H^{1/2}(\partial O)} = +\infty.$$

The Linear Sampling Method consists then, for all $z \in \mathscr{G}$, where $\mathscr{G}$ is a sampling grid of W, in solving a regularized version of the near-field equation $N\hat{h} = G(\cdot, z)|_{\hat{\Sigma}}$. Following [3], we introduce a modal formulation of the Linear Sampling Method: the principle is to project such near-field equation on the complete basis $(\theta_n)_{n\in\mathbb{N}}$ of the transverse section Σ_{-R} and on the complete basis $(\tilde{\theta}_n)_{n\in\mathbb{N}}$ of the transverse section $\tilde{\Sigma}_R$. This enables us to propose a "physical regularization" which consists in replacing the series which result from these projections by the sum of their first P or $\tilde{P}$ terms. This amounts to keep, among the information contained in the incident and scattered waves, their propagating parts only, in other words to neglect their evanescent parts. We need the following proposition.

Lemma 2.2. *We have*

$$u^s(x, y) = \begin{cases} -\displaystyle\sum_{n\in\mathbb{N}} \frac{1}{2i\beta_n} u_n^s(x) g_n^-(y) & for \quad y_3 = -R,\ x_3 > -R \\ -\displaystyle\sum_{n\in\mathbb{N}} \frac{1}{2i\tilde{\beta}_n} \tilde{u}_n^s(x) \tilde{g}_n^+(y) & for \qquad y_3 = R,\ x_3 < R, \end{cases}$$

where u_n^s and $\tilde{u}_n^s$ are the solutions to problem (23) for $f = -u_n|_{\partial O}$ and $f = -\tilde{u}_n|_{\partial O}$, respectively, while u_n and $\tilde{u}_n$ are the solutions to problems (5) and (6), respectively.

Proof. Let us consider the case $y_3 = -R$ and $x_3 > -R$, the other case is similar. From Proposition 3, we have

$$G(x, y) = -\sum_{n\in\mathbb{N}} \frac{1}{2i\beta_n} u_n(x) g_n^-(y).$$

By linearity of problem (23) with respect to the Dirichlet data f, we obtain that

$$u^s(x,y) = -\sum_{n\in\mathbb{N}} \frac{1}{2i\beta_n} u_n^s(x) g_n^-(y),$$

which is the result. □

From Lemma 2.2 and from Proposition 3, a straightforward computation shows that the operator N and the test function $G(\cdot,z)|_{\tilde{\Sigma}}$ in the full-scattering case have the following explicit expressions in the form of series.

Proposition 6. *For $\hat{h} = (h, \tilde{h}) \in L^2(\Sigma_{-R}) \times L^2(\tilde{\Sigma}_R)$, $(N\hat{h}) \in L^2(\Sigma_{-R}) \times L^2(\tilde{\Sigma}_R)$ is given by*

$$(N\hat{h})(x) = \begin{cases} -\displaystyle\sum_{m\in\mathbb{N}}\sum_{n\in\mathbb{N}} \left(\frac{e^{i\beta_n R}}{2i\beta_n} (U_n)_m^- h_n + \frac{e^{i\tilde{\beta}_n R}}{2i\tilde{\beta}_n} (\tilde{U}_n)_m^- \tilde{h}_n \right) \theta_m(x_S) & \text{for} \quad x \in \Sigma_{-R} \\ -\displaystyle\sum_{m\in\mathbb{N}}\sum_{n\in\mathbb{N}} \left(\frac{e^{i\beta_n R}}{2i\beta_n} (U_n)_m^+ h_n + \frac{e^{i\tilde{\beta}_n R}}{2i\tilde{\beta}_n} (\tilde{U}_n)_m^+ \tilde{h}_n \right) \tilde{\theta}_m(x_S) & \text{for} \quad x \in \tilde{\Sigma}_R, \end{cases}$$

where we have used the decompositions

$$h = \sum_{n\in\mathbb{N}} h_n \theta_n, \quad \tilde{h} = \sum_{n\in\mathbb{N}} \tilde{h}_n \tilde{\theta}_n$$

and

$$\begin{cases} u_n^s(x) = \displaystyle\sum_{m\in\mathbb{N}} (U_n)_m^- \theta_m(x_S) \quad \tilde{u}_n^s(x) = \sum_{m\in\mathbb{N}} (\tilde{U}_n)_m^- \theta_m(x_S) & \text{for} \quad x \in \Sigma_{-R} \\ u_n^s(x) = \displaystyle\sum_{m\in\mathbb{N}} (U_n)_m^+ \tilde{\theta}_m(x_S) \quad \tilde{u}_n^s(x) = \sum_{m\in\mathbb{N}} (\tilde{U}_n)_m^+ \tilde{\theta}_m(x_S) & \text{for} \quad x \in \tilde{\Sigma}_R. \end{cases}$$

Proposition 7. *For $x \in \Sigma_{-R}$ and $z \in W_R^b$,*

$$G(x,z) = \begin{cases} -\displaystyle\sum_{m\in\mathbb{N}}\sum_{n\in\mathbb{N}} \frac{e^{-i\beta_n z_3}}{2i\beta_n} (u_n, \theta_m)_{L^2(\Sigma_{-R})} \theta_n(z_S)\theta_m(x_S) \\ \quad -\displaystyle\sum_{m\in\mathbb{N}} \frac{1}{2i\beta_m} (e^{i\beta_m(R+z_3)} - e^{-i\beta_m(R+z_3)}) \theta_m(z_S)\theta_m(x_S) & \text{for} \quad z_3 \in (-R, 0) \\ -\displaystyle\sum_{m\in\mathbb{N}}\sum_{n\in\mathbb{N}} \frac{e^{i\tilde{\beta}_n z_3}}{2i\tilde{\beta}_n} (\tilde{u}_n, \theta_m)_{L^2(\Sigma_{-R})} \tilde{\theta}_n(z_S)\theta_m(x_S) & \text{for} \quad z_3 \in (0, R), \end{cases}$$

for $x \in \tilde{\Sigma}_R$ and $z \in W_R^b$,

$$G(x,z) = \begin{cases} -\displaystyle\sum_{m\in\mathbb{N}}\sum_{n\in\mathbb{N}} \frac{e^{-i\beta_n z_3}}{2i\beta_n} (u_n, \tilde{\theta}_m)_{L^2(\tilde{\Sigma}_R)} \theta_n(z_S)\tilde{\theta}_m(x_S) & \text{for} \quad z_3 \in (-R, 0) \\ -\displaystyle\sum_{m\in\mathbb{N}}\sum_{n\in\mathbb{N}} \frac{e^{i\tilde{\beta}_n z_3}}{2i\tilde{\beta}_n} (\tilde{u}_n, \tilde{\theta}_m)_{L^2(\tilde{\Sigma}_R)} \tilde{\theta}_n(z_S)\tilde{\theta}_m(x_S) \\ \quad -\displaystyle\sum_{m\in\mathbb{N}} \frac{1}{2i\tilde{\beta}_m} (e^{i\tilde{\beta}_m(R-z_3)} - e^{-i\tilde{\beta}_m(R-z_3)}) \tilde{\theta}_m(z_S)\tilde{\theta}_m(x_S) & \text{for} \quad z_3 \in (0, R), \end{cases}$$

where u_n and $\tilde{u}_n$ are the solutions to problems (5) and (6), respectively.

We complete Proposition 7 with an alternative and simpler expression of the test function $G(\cdot,z)|_{\hat{\Sigma}}$, which is obtained by using the reciprocity relationship satisfied by the fundamental solution G, that is $G(x,y)=G(y,x)$ for all $(x,y)\in W\times W$.

Proposition 8. *For $x\in\Sigma_{-R}$ and $z\in W_R^b$,*

$$G(x,z)=-\sum_{m\in\mathbb{N}}\frac{e^{i\beta_m R}}{2i\beta_m}u_m(z)\theta_m(x_S).$$

For $x\in\tilde{\Sigma}_R$ and $z\in W_R^b$,

$$G(x,z)=-\sum_{m\in\mathbb{N}}\frac{e^{i\tilde{\beta}_m R}}{2i\tilde{\beta}_m}\tilde{u}_m(z),\tilde{\theta}_m(x_S).$$

Here, u_n and $\tilde{u}_n$ are the solutions to problems (5) and (6), respectively.

Proof. Let us assume that $x\in\Sigma_{-R}$ and $z\in W_R^b$. From the reciprocity relationship, we have $G(x,z)=G(z,x)$ and from the formula (18) given that $z_3>x_3$, we get

$$G(z,x)=-\sum_{m\in\mathbb{N}}\frac{1}{2i\beta_m}g_m^-(x)u_m(z)=-\sum_{m\in\mathbb{N}}\frac{e^{i\beta_m R}}{2i\beta_m}u_m(z)\theta_m(x_S).$$

The case $x\in\tilde{\Sigma}_R$ and $z\in W_R^b$ would be addressed the same way. □

Remark 3. It is important to note that:

- in the full-scattering case, it is equivalent to measure $u^s(x,y)$ for all $(x,y)\in\Sigma_{-R}\cup\tilde{\Sigma}_R$ and to measure all the projections of the fields u_n^s and $\tilde{u}_n^s$ on the transverse functions θ_m of Σ_{-R} and on the transverse functions $\tilde{\theta}_m$ of $\tilde{\Sigma}_R$, with $m,n\in\mathbb{N}$,
- in the back-scattering case, it is equivalent to measure $u^s(x,y)$ for all $(x,y)\in\Sigma_{-R}$ and to measure all the projections of the fields u_n^s on the transverse functions θ_m of Σ_{-R}, with $m,n\in\mathbb{N}$.

By restricting the series to P (section Σ_{-R}) or $\tilde{P}$ (section $\tilde{\Sigma}_R$) terms in Propositions 6 and 7, in the full-scattering case the near-field equation $N\hat{h}=G(\cdot,z)|_{\hat{\Sigma}}$ boils down to the finite square system

$$\begin{pmatrix}A^- & \tilde{A}^-\\ A^+ & \tilde{A}^+\end{pmatrix}\begin{pmatrix}H^-\\ H^+\end{pmatrix}=\begin{pmatrix}D^-(z)\\ D^+(z)\end{pmatrix},\tag{26}$$

where the matrices $A^-\in\mathbb{C}^{P\times P}$, $\tilde{A}^-\in\mathbb{C}^{P\times\tilde{P}}$, $A^+\in\mathbb{C}^{\tilde{P}\times P}$ and $\tilde{A}^+\in\mathbb{C}^{\tilde{P}\times\tilde{P}}$ are given by

$$\begin{cases}A^-_{mn}=\dfrac{e^{i\beta_n R}}{2i\beta_n}(U_n)^-_m, \quad \tilde{A}^-_{mn}=\dfrac{e^{i\tilde{\beta}_n R}}{2i\tilde{\beta}_n}(\tilde{U}_n)^-_m,\\ A^+_{mn}=\dfrac{e^{i\beta_n R}}{2i\beta_n}(U_n)^+_m, \quad \tilde{A}^+_{mn}=\dfrac{e^{i\tilde{\beta}_n R}}{2i\tilde{\beta}_n}(\tilde{U}_n)^+_m,\end{cases}\tag{27}$$

where the vectors $H^-\in\mathbb{C}^P$ and $H^+\in\mathbb{C}^{\tilde{P}}$ are given by

$$H^-_n=h_n, \quad H^+_n=\tilde{h}_n,\tag{28}$$

and where the vectors $D^- \in \mathbb{C}^P$ and $D^+ \in \mathbb{C}^{\tilde{P}}$ are given by the following formulas. For $m = 0, \dots, P-1$,

$$D_m^-(z) = \begin{cases} \displaystyle\sum_{n=0}^{P-1} \frac{e^{-i\beta_n z_3}}{2i\beta_n} (u_n, \theta_m)_{L^2(\Sigma_{-R})} \theta_n(z_S) \\ \quad + \dfrac{1}{2i\beta_m} (e^{i\beta_m(R+z_3)} - e^{-i\beta_m(R+z_3)}) \theta_m(z_S) & \text{for} \quad z_3 \in (-R, 0) \\ \displaystyle\sum_{n=0}^{\tilde{P}-1} \frac{e^{i\tilde{\beta}_n z_3}}{2i\tilde{\beta}_n} (\tilde{u}_n, \theta_m)_{L^2(\Sigma_{-R})} \tilde{\theta}_n(z_S) & \text{for} \quad z_3 \in (0, R). \end{cases} \tag{29}$$

For $m = 0, \dots, \tilde{P}-1$,

$$D_m^+(z) = \begin{cases} \displaystyle\sum_{n=0}^{P-1} \frac{e^{-i\beta_n z_3}}{2i\beta_n} (u_n, \tilde{\theta}_m)_{L^2(\tilde{\Sigma}_R)} \theta_n(z_S) & \text{for} \quad z_3 \in (-R, 0) \\ \displaystyle\sum_{n=0}^{\tilde{P}-1} \frac{e^{i\tilde{\beta}_n z_3}}{2i\tilde{\beta}_n} (\tilde{u}_n, \tilde{\theta}_m)_{L^2(\tilde{\Sigma}_R)} \tilde{\theta}_n(z_S) \\ \quad + \dfrac{1}{2i\tilde{\beta}_m} (e^{i\tilde{\beta}_m(R-z_3)} - e^{-i\tilde{\beta}_m(R-z_3)}) \tilde{\theta}_m(z_S) & \text{for} \quad z_3 \in (0, R). \end{cases} \tag{30}$$

Using Proposition 8 instead of Proposition 7, alternative formulas for $D_m^-(z)$ and $D_m^+(z)$ are the following. For $m = 0, \dots, P-1$,

$$D_m^-(z) = \frac{e^{i\beta_m R}}{2i\beta_m} u_m(z), \tag{31}$$

while for $m = 0, \dots, \tilde{P}-1$,

$$D_m^+(z) = \frac{e^{i\tilde{\beta}_m R}}{2i\tilde{\beta}_m} \tilde{u}_m(z). \tag{32}$$

We readily see that in the back-scattering case, the near-field equation simply becomes

$$A^- H^- = D^-(z). \tag{33}$$

Remark 4. It is interesting to note that in the formulas (29) and (30), $D_m^-(z)$ and $D_m^+(z)$ only depend on the values of the reference fields u_n and $\tilde{u}_n$ on the transverse sections Σ_{-R} and $\tilde{\Sigma}_R$, so that these values could be themselves experimental data (that is the responses of the waveguide without the obstacle). In contrast, in the formulas (31) and (32), $D_m^-(z)$ and $D_m^+(z)$ depend on the values of the reference fields in the whole sampling grid, which means that they cannot be obtained experimentally, rather numerically.

3 A waveguide with a transition zone

As mentioned in the introduction, in order to image a weld bead, we consider a transition zone between two half-waveguides. The domain W now consists of three domains, a left half-waveguide $W_{-R} = S \times (-\infty, -R)$, a right half-waveguide

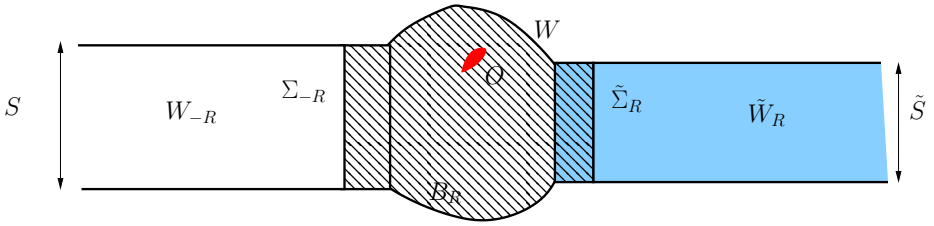

Figure 3: A waveguide with a transition zone (the domain B_R is hatched)

$\tilde{W}_R = \tilde{S} \times (R, +\infty)$ and a bounded domain B_R in between, the transverse section $\Sigma_{-R} = S \times \{-R\}$ separating the domains W_{-R} and B_R, the transverse section $\tilde{\Sigma}_R = \tilde{S} \times \{R\}$ separating the domains B_R and $\tilde{W}_R$. It should be noted (see Figure 3) that the domain B_R contains a finite part of the half-waveguides W_{R_0} and $\tilde{W}_{-R_0}$, $R_0 < R$. The refractive index $\eta \in L^\infty(W)$ is again constant in W_{-R_0} and in $\tilde{W}_{R_0}$, with $\eta(x) = 1$ for $x \in W_{-R_0}$ and $\eta(x) = \tilde{n}$ for $x \in \tilde{W}_{R_0}$. This in particular implies that $\eta(x) = 1$ for $x \in W_{-R}$ and $\eta(x) = \tilde{n}$ for $x \in \tilde{W}_R$. For this waveguide W with a junction, for $n \in \mathbb{N}$ we can as previously define $g^+_{n,0}$ as the extension of g^+_n in W_{-R} by 0 in $B_R \cup \tilde{W}_R$ and $\tilde{g}^-_{n,0}$ as the extension of $\tilde{g}^-_n$ in $\tilde{W}_R$ by 0 in $B_R \cup W_{-R}$. We now introduce the reference fields u_n and $\tilde{u}_n$ defined by problems (5) and (6) for $n \in \mathbb{N}$ and the fundamental solution $G(\cdot, y)$ defined by problem (17) for $y \in W$. If the point y belongs to a straight part of the domain W, we have simple expressions for $G(\cdot, y)$ in terms of the reference fields.

Proposition 9. *The fundamental solution $G(\cdot, y)$ has the following properties:*

- *for $y \in W_{-R}$ and $x \in W$ with $x_3 > -R$,*

$$G(x, y) = -\sum_{n \in \mathbb{N}} \frac{1}{2i\beta_n} g^-_n(y) u_n(x),$$

- *for $y \in \tilde{W}_R$ and $x \in W$ with $x_3 < R$,*

$$G(x, y) = -\sum_{n \in \mathbb{N}} \frac{1}{2i\tilde{\beta}_n} \tilde{g}^+_n(y) \tilde{u}_n(x),$$

where u_n and $\tilde{u}_n$ are the solutions to problems (5) and (6), respectively.

Proof. The proof is very close to the one of Proposition 3. We only consider the case when $y \in W_{-R}$ and $x \in W$ with $x_3 > -R$ (the other case is similar). We again use the decomposition $G(\cdot, y) = \mathcal{G}_0(\cdot, y) + \mathcal{G}^s(\cdot, y)$, where $\mathcal{G}_0(\cdot, y)$ is the extension of $\mathcal{G}(\cdot, y)$ in W_{-R} by 0 in $B_R \cup \tilde{W}_R$. The field $\mathcal{G}^s(\cdot, y)$ satisfies the transmission problem

$$\begin{cases} \Delta \mathcal{G}^s(\cdot, y) + k^2 \eta^2 \mathcal{G}^s(\cdot, y) = 0 & \text{in} \quad W_{-R} \cup B_R \cup \tilde{W}_R \\ \partial_\nu \mathcal{G}^s(\cdot, y) = 0 & \text{on} \quad \partial W \\ [\![\mathcal{G}^s(\cdot, y)]\!] = \mathcal{G}(\cdot, y) & \text{on} \quad \Sigma_{-R} \\ [\![\partial_{x_3} \mathcal{G}^s(\cdot, y)]\!] = \partial_{x_3} \mathcal{G}(\cdot, y) & \text{on} \quad \Sigma_{-R} \\ [\![\mathcal{G}^s(\cdot, y)]\!] = 0 & \text{on} \quad \tilde{\Sigma}_R \\ [\![\partial_{x_3} \mathcal{G}^s(\cdot, y)]\!] = 0 & \text{on} \quad \tilde{\Sigma}_R \\ \mathcal{G}^s(\cdot, y) & \text{is outgoing.} \end{cases} \tag{34}$$

We now use the decomposition $u_n = g^+_{n,0} + v^s_n$ for all $n \in \mathbb{N}$. The field v^s_n satisfies the transmission problem

$$\begin{cases} \Delta v^s_n + k^2\eta^2 v^s_n = 0 & \text{in} \quad W_{-R} \cup B_R \cup \tilde{W}_R \\ \partial_\nu v^s_n = 0 & \text{on} \quad \partial W \\ [\![v^s_n]\!] = g^+_n & \text{on} \quad \Sigma_{-R} \\ [\![\partial_{x_3} v^s_n]\!] = \partial_{x_3} g^+_n & \text{on} \quad \Sigma_{-R} \\ [\![v^s_n]\!] = 0 & \text{on} \quad \tilde{\Sigma}_R \\ [\![\partial_{x_3} v^s_n]\!] = 0 & \text{on} \quad \tilde{\Sigma}_R \\ v^s_n(\cdot, y) & \text{is outgoing.} \end{cases} \tag{35}$$

Since $x_3 > y_3$ we have

$$\mathcal{G}(x,y) = -\sum_{n\in\mathbb{N}} \frac{1}{2i\beta_n} g^-_n(y) g^+_n(x),$$

which in view of the systems (34) and (35) implies that

$$\mathcal{G}^s(x,y) = -\sum_{n\in\mathbb{N}} \frac{1}{2i\beta_n} g^-_n(y) v^s_n(x).$$

We complete the proof observing that in $B_R \cup \tilde{W}_R$, we have $g^+_{n,0} = 0$ and $\mathcal{G}_0(\cdot, y) = 0$, that is $u_n = v^s_n$ and $G(\cdot, y) = \mathcal{G}^s(\cdot, y)$. □

Remark 5. We note that in contrast with Proposition 3, a closed-form expression for $G(x,y)$ is not given in Proposition 9 for all $(x,y) \in W \times W$.

We now introduce an obstacle within the domain W, more precisely in B_R, denoting again $\Omega = W \backslash \overline{O}$. Once again we define the solutions $u(\cdot, y)$ and $u^s(\cdot, y)$ to problems (22) and (23), for all $y \in \Omega$. We also introduce the operators N and H defined by (24) and (25). Then Theorem 2.1, Lemma 2.2 and Proposition 6 still hold (in particular, Lemma 2.2 is now a consequence of Proposition 9). However, Proposition 7 is not valid any more. Using again the reciprocity relationship satisfied by the fundamental solution G, we get the following proposition, which is the analogous of Proposition 8.

Proposition 10. *For $x \in \Sigma_{-R}$ and $z \in B_R$,*

$$G(x,z) = -\sum_{m\in\mathbb{N}} \frac{e^{i\beta_m R}}{2i\beta_m} u_m(z)\theta_m(x_S),$$

for $x \in \tilde{\Sigma}_R$ and $z \in B_R$,

$$G(x,z) = -\sum_{m\in\mathbb{N}} \frac{e^{i\tilde{\beta}_m R}}{2i\tilde{\beta}_m} \tilde{u}_m(z)\tilde{\theta}_m(x_S),$$

where u_n and $\tilde{u}_n$ are the solutions to problems (5) and (6), respectively.

By restricting the series to P or $\tilde{P}$ terms, in the full-scattering case the near-field equation $N\hat{h} = G(\cdot, z)|_{\hat{\Sigma}}$ now amounts to the finite system

$$\begin{pmatrix} A^- & \tilde{A}^- \\ A^+ & \tilde{A}^+ \end{pmatrix} \begin{pmatrix} H^- \\ H^+ \end{pmatrix} = \begin{pmatrix} D^-(z) \\ D^+(z) \end{pmatrix},$$

where the matrices A^-, $\tilde{A}^-$, A^+ and $\tilde{A}^+$ are given by (27), the vectors H^- and H^+ are given by (28), and the vectors $D^-(z)$ and $D^+(z)$ are given by (31) and (32), respectively. In the back-scattering case, the near-field equation $N\hat{h} = G(\cdot, z)|_{\hat{\Sigma}}$ reduces to the finite system

$$A^- H^- = D^-(z).$$

4 Extension to a junction of several half-waveguides

In the previous section we have addressed the Linear Sampling Method to image a junction between two half-waveguides. In the present section we wish to extend such method to a junction of a finite number M of half-waveguides. Since the justifications are the same as for the case $M = 2$, we skip them. However we have to introduce some notations. The union of the junction and all half-waveguides is denoted W and is characterized by a refractive index $\eta \in L^\infty(W)$. Each half-waveguide W^j, $j = 0, \ldots, M-1$, has a constant section S^j and a constant refractive index η^j. We introduce the eigenvalues and eigenfunctions $(\lambda_n^j, \theta_n^j)_{n\in\mathbb{N}}$ of the transverse problem (2) associated to the section S^j of half-waveguide W^j. Denoting $\kappa^j = k\eta^j$, the corresponding wave numbers β_n^j are computed following (3) by replacing κ by κ^j and λ_n by λ_n^j. The junction is a bounded domain B such that

$$W = B \cup \bigcup_{j=0}^{M-1} W^j.$$

Each half-waveguide W^j has its own local set of coordinates $x = (x_S, x_3)$, where x_3 is oriented from infinity to the junction, so that $W^j = S^j \times (-\infty, -R^j)$. The support of emitters and receivers, again denoted $\hat{\Sigma}$, is defined by

$$\hat{\Sigma} = \prod_{j=0}^{M-1} \Sigma^j,$$

where Σ^j is the transverse section of the half-waveguide W^j of local coordinate $x_3 = -R^j$. Some of the previous notations are illustrated on figure 4 for $M = 3$. For $j = 0, \ldots, M-1$ and $n \in \mathbb{N}$, the guided mode g_n^j which propagates or exponentially decreases in the half-waveguide W_j from infinity to the junction satisfies

$$g_n^j(x) = e^{i\beta_n^j x_3} \theta_n^j(x_S).$$

The number of propagating modes in the half-waveguide W_j is denoted $P(j)$. To each of such guided mode g_n^j we can associate a reference field u_n^j via problem (5), by replacing g_n^+ by g_n^j. Similarly, for any $y \in W$ we define the fundamental solution $G(\cdot, y)$ via problem (17). Let us now assume that there is a Dirichlet obstacle O to retrieve in the junction B. For all $y \in W$, we introduce the total field

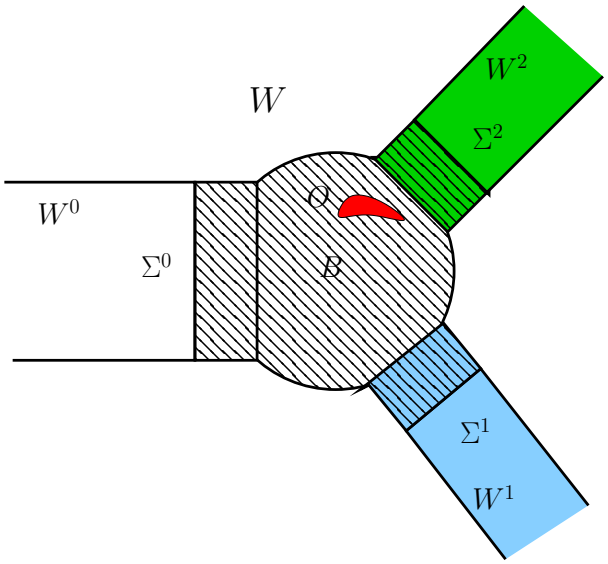

Figure 4: A junction of three half-waveguides (the domain B is hatched)

$u(\cdot, y)$ which satisfies (22) and the scattered field $u^s(\cdot, y)$ which satisfies (23) with $f = -G(\cdot, y)|_{\partial O}$. For $j = 0, \ldots, M-1$ and $n \in \mathbb{N}$, the solution to the problem (23) for $f = -u_n^j|_{\partial O}$ is denoted $u_n^{s,j}$. The near-field equation in the full-scattering case is: for each $z \in \mathscr{G}$, which is a sampling grid of B, find $\hat{h} \in \hat{\Sigma}$ such that

$$\left(\int_{\hat{\Sigma}} u^s(\cdot, y) \hat{h}(y)\, ds(y) \right) |_{\hat{\Sigma}} = G(\cdot, z)|_{\hat{\Sigma}}.$$

In what follows, the index e refers to the emitter, the index r to the receiver. The above near-field equation also reads: for $r = 0, \ldots, M-1$ and $x \in \Sigma^r$ find $(h^0, h^1, \ldots, h^{M-1}) \in \Sigma^0 \times \Sigma^1 \times \ldots \times \Sigma^{M-1}$ such that

$$\sum_{e=0}^{M-1} \int_{\Sigma^e} u^s(x, y) h^e(y)\, ds(y) = G(x, z). \tag{36}$$

Let us give some explicit expression of the left-hand side of the near-field equation (36). By proceeding as in Lemma 2.2, for $y \in \Sigma^e$ and $x \in B$, we get

$$u^s(x, y) = -\sum_{n \in \mathbb{N}} \frac{e^{i\beta_n^e R^e}}{2i\beta_n^e} u_n^{s,e}(x) \theta_n^e(y_S),$$

which by denoting for $e, r = 0, \ldots, M-1$ and $n \in \mathbb{N}$,

$$u_n^{s,e}|_{\Sigma^r} = \sum_{m \in \mathbb{N}} (U_n^e)_m^r \theta_m^r \quad \text{and} \quad h^e = \sum_{m \in \mathbb{N}} h_m^e \theta_m^e,$$

implies that for $r = 0, \ldots, M-1$ and $x \in \Sigma^r$,

$$\sum_{e=0}^{M-1} \int_{\Sigma^e} u^s(x, y) h^e(y)\, ds(y) = -\sum_{e=0}^{M-1} \sum_{m \in \mathbb{N}} \sum_{n \in \mathbb{N}} \frac{e^{i\beta_n^e R^e}}{2i\beta_n^e} (U_n^e)_m^r h_n^e \theta_m^r(x_S).$$

Let us now give an explicit expression of the right-hand side of (36). For $r = 0, \dots, M-1$ and $x \in \Sigma^r$, for all $z \in \mathscr{G}$, using again the reciprocity relationship we get

$$G(x,z) = G(z,x) = -\sum_{m\in\mathbb{N}} \frac{e^{i\beta_m^r R^r}}{2i\beta_m^r} u_m^r(z)\theta_m^r(x_S).$$

Finally, if we restrict the series to the number of propagating modes in each half-waveguide, we obtain the following discrete near-field equation: for $r = 0, \dots, M-1$, for $m = 0, \dots, P(r)-1$,

$$\sum_{e=0}^{M-1} \sum_{n=0}^{P(e)-1} \frac{e^{i\beta_n^e R^e}}{2i\beta_n^e} (U_n^e)_m^r h_n^e = \frac{e^{i\beta_m^r R^r}}{2i\beta_m^r} u_m^r(z). \tag{37}$$

Remark 6. From the system (37), which corresponds to the full-scattering data, it is very easy to deduce the one obtained for partial data, that is when emitters and receivers are located on strictly less than M transverse sections Σ^j.

5 Numerical experiments

5.1 Introduction

In order to show some $2D$ numerical experiments of the inverse problem, we compute artificial data by solving the forward scattering problems (23) in a bounded domain with the help of Dirichlet-to-Neumann operators on each half-waveguide and by using a Finite Element Method. This enables us to construct the matrices A^-, A^+, $\tilde{A}^-$ and $\tilde{A}^+$ defined by (27) and the corresponding matrices in the case of the extension to a junction of several half-waveguides (see the left-hand side of (37)). In all the experiments conducted in the sequel, the identification results are presented for exact data (the data are exactly the scattered fields obtained by the FEM) and for noisy data. Noisy data are obtained following the method described in [3]. Indeed, let us consider the trace on a transverse section Σ of a scattered field u^s obtained with the FEM. We compute, with the help of a subdivision of Σ into a finite number of intervals, a pointwise Gaussian noise b. The noisy data u_δ^s is then defined on Σ by

$$u_\delta^s = u^s + \alpha\, b,$$

where the real number $\alpha > 0$ is calibrated in such a way that

$$\|u_\delta^s - u^s\|_{L^2(\Sigma)} = 0.1\, \|u^s\|_{L^2(\Sigma)},$$

which means that our relative amplitude of noise is 10%. For $z \in \mathscr{G}$, let us denote

$$AH = D(z) \tag{38}$$

either the $(P+\tilde{P}) \times (P+\tilde{P})$ full-scattering system (26) or the $P \times P$ back-scattering system (33) for a junction of two half-waveguides. In the case of exact data A, we exactly solve (38). In the presence of noisy data A_δ, with $|||A_\delta - A||| \leqslant \delta$, where $|||\cdot|||$ is a matrix norm, we solve the Tikhonov equation associated with (38), that is

$$(A_\delta^* A_\delta)H + \varepsilon H = A_\delta^* D(z), \tag{39}$$

where A_δ^* is the adjoint of A_δ and $\varepsilon > 0$. Following exactly [22] and as in [3], for a given point z, the regularization parameter ε is uniquely determined as a function of δ according to the Morozov's discrepancy principle. More precisely, we compute ε by using a singular value decomposition of A_δ and a simple dichotomy method. It remains to construct the right-hand side of (26), or (37) in the case of the extension to a junction of several half-waveguides. This is done by using formulas (31) and (32), which require to compute the reference fields u_n and $\tilde{u}_n$ (they satisfy (5) and (6)) and the corresponding fields in the case of the extension to a junction of several half-waveguides (see the right-hand side of (37)). Unless we consider a straight waveguide (see Proposition 4), these reference fields have to be computed numerically by using a FEM. A crucial point is that those reference fields are independent of z and of the obstacle O. They are hence computed once and for all, which is important as regards the efficiency of the Linear Sampling Method in this context. In comparison with the case of a straight and homogeneous waveguide, the computational cost is increased by the preliminary FEM computations of the reference fields, in particular if the junction domain is large. In all the pictures presented hereafter, we show the level sets of the function

$$\psi(z) = \log\left(\frac{1}{\|H(z)\|}\right),$$

where $H(z)$ is the solution to (38) for exact data and the solution to (39) for noisy data, such solution depending implicitly on z. Here $\|\cdot\|$ denotes a L^2 discrete norm. In view of Theorem 2.1, $\psi(z)$ is almost $-\infty$ unless $z \in O$, which means that the level sets of ψ almost characterize the obstacle.

5.2 Waveguide with an abrupt change of refractive index

We consider the particular case of section 2 when the waveguide is straight, that is $S = \tilde{S}$, but characterized by an abrupt change of refractive index, that is $\kappa \neq \tilde{\kappa}$. Here we have $h = \tilde{h} = 1$, while $R = 1$. We consider four kinds of obstacle.

1. A square within the left half-waveguide W_0.
2. A circle within the right half-waveguide $\tilde{W}_0$.
3. The union of the two previous obstacles.
4. A triangle at the interface of half-waveguides W_0 and $\tilde{W}_0$.

In figure 5, we show the identification result for obstacle 3 and obstacle 4 in the full-scattering case, with wave number $\kappa = 40$ in the left half-waveguide W_0 and $\tilde{\kappa} = 60$ in the right half-waveguide $\tilde{W}_0$. The corresponding number of propagating modes are $P = 13$ and $\tilde{P} = 20$, respectively. We observe that the quality of the images are as good as if the waveguide were homogeneous. Next, in figures 6, 7 and 8, we present the identification results in the back-scattering case for obstacle 1 (obstacle in the half-waveguide which supports the data), obstacle 2 (obstacle in the half-waveguide which does not support the data) and obstacle 4 (obstacle at the interface), respectively. For each of these obstacles, we show the obtained images when $(\kappa, \tilde{\kappa}) = (40, 20)$, $(\kappa, \tilde{\kappa}) = (40, 40)$ and $(\kappa, \tilde{\kappa}) = (40, 60)$. We can draw two kinds of conclusion. Firstly, as expected the obstacle is better retrieved when it is located in the half-waveguide which supports the data because the identification

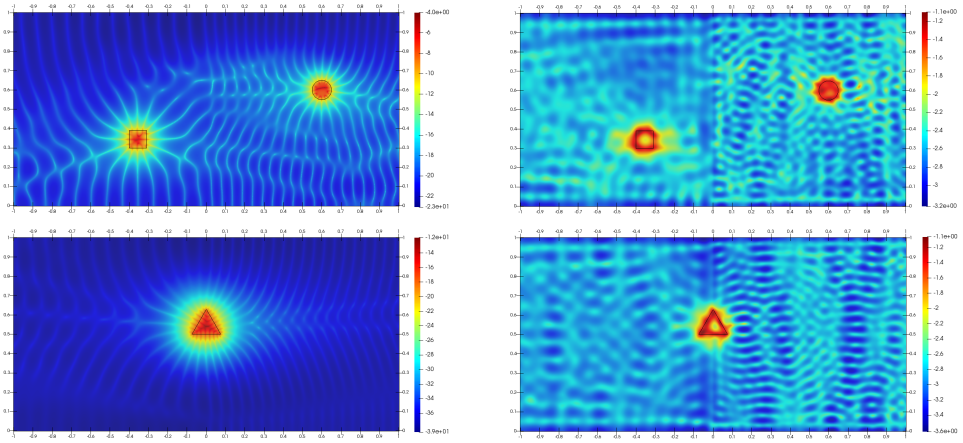

Figure 5: Full-scattering, $\kappa = 40$ ($P = 13$) and $\tilde{\kappa} = 60$ ($\tilde{P} = 20$). Top left: obstacle 3 and exact data. Top right: obstacle 3 and noisy data. Bottom left: obstacle 4 and exact data. Bottom right: obstacle 4 and noisy data.

benefits from the reflected waves by the interface between the two half-waveguides. Secondly, in the case when the obstacle lies in the half-waveguide which does not support the data, we observe that the obstacle is not better retrieved if $\tilde{\kappa}$ is larger than κ instead of being equal to κ. This could seem paradoxical, in the sense that the larger is the wave number, the bigger is the number of propagating modes and hence the better should be the resolution. This can be interpreted, in view of Proposition 4, as follows: the P propagating modes g_n^+ in W_0 are transmitted in $\tilde{W}_0$ in the form of the modes $\tilde{g}_n^+$, so that only P propagating modes in $\tilde{W}_0$ among their total number $\tilde{P} > P$ are excited, the remainder $(\tilde{P} - P)$ are not.

5.3 Waveguide with an abrupt change of section

We now consider the particular case of section 2 when the refractive index is uniform, that is $\kappa = \tilde{\kappa}$, but the waveguide is characterized by an abrupt change of section, that is $S \neq \tilde{S}$. In figure 9, we show the identification result for obstacle 3 in the full-scattering case, with $\kappa = \tilde{\kappa} = 40$, but $h \neq \tilde{h}$, that is $h = 0.65$ and $\tilde{h} = 1$. The corresponding numbers of propagating modes are $P = 9$ and $\tilde{P} = 13$. Again we observe that the quality of the images are as good as if the waveguide were straight. Now we consider the back-scattering case when the obstacle lies in the half-waveguide which supports the data (obstacle 1), in the particular case $h/\tilde{h} > 1$ in figure 10 and $h/\tilde{h} < 1$ in figure 11. The interpretation of these results is quite clear. For $h = 1$, the identification results are better if $\tilde{h} = 0.5$ than if $\tilde{h} = 0.75$ (figure 10), because the amount of reflected waves at the interface between the two half-waveguides is larger (at the limit when $\tilde{h}$ tends to 0, our waveguide tends to a terminating waveguide like in [13], which can be seen as an ideal situation). On the contrary, for $\tilde{h} = 1$, the identification results are better if $h = 0.75$ than if $h = 0.5$ (figure 11), because the number of incident propagating modes in W_0 is larger in the first case. Next we consider the back-scattering case when the obstacle lies in the half-waveguide which does not support the data (obstacle 2), in the particular case $h/\tilde{h} > 1$ in figure 12 and $h/\tilde{h} < 1$ in figure 13. For $h = 1$, the identification

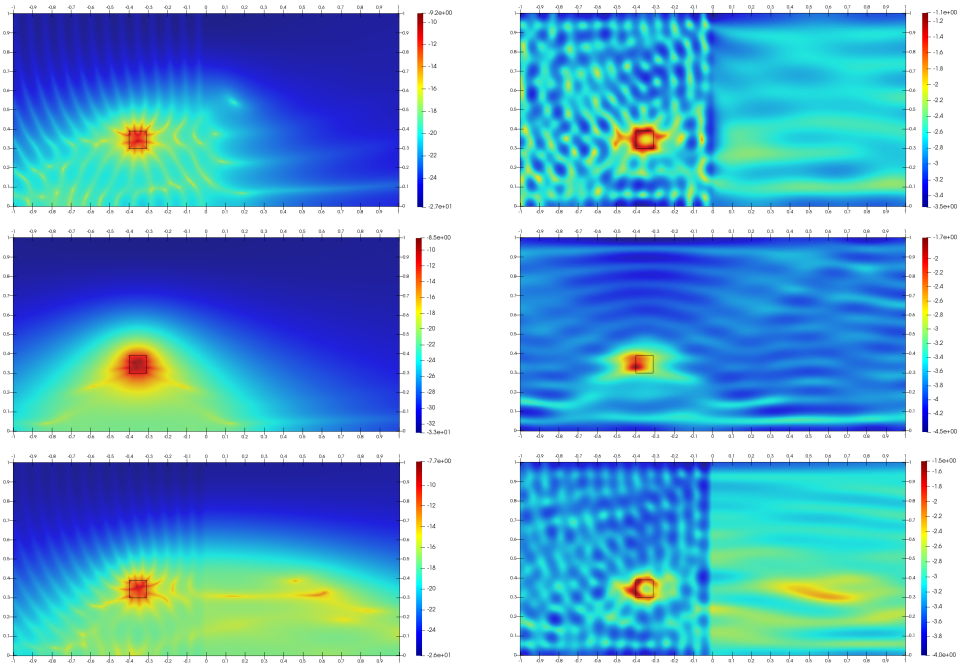

Figure 6: Back-scattering for obstacle 1. Top left: $\kappa = 40$ ($P = 13$) and $\tilde{\kappa} = 20$ ($\tilde{P} = 7$), exact data. Top right: $\kappa = 40$ and $\tilde{\kappa} = 20$, noisy data. Middle left: $\kappa = \tilde{\kappa} = 40$ ($P = \tilde{P} = 13$), exact data. Middle right: $\kappa = \tilde{\kappa} = 40$, noisy data. Bottom left: $\kappa = 40$ ($P = 13$) and $\tilde{\kappa} = 60$ ($\tilde{P} = 20$), exact data. Bottom right: $\kappa = 40$ and $\tilde{\kappa} = 60$, noisy data.

results are better if $\tilde{h} = 0.75$ than if $\tilde{h} = 0.5$ (figure 12), because the amount of reflected waves increases while the amount of transmitted waves that reach the obstacle decreases, which deteriorates the quality of the identification. For $\tilde{h} = 1$, the identification results are better if $h = 0.75$ than if $h = 0.5$ (figure 13), because the number of incident propagating modes in W_0 is larger in the first case, and they are all transmitted in the form of propagating modes in $\tilde{W}_0$ because $\tilde{P} > P$.

5.4 Junction of three waveguides

To complete the numerical experiments, we present some identification results in the case of a junction of three half-waveguides presented in section 4 (see figure 4, which shows the position of the three half-waveguides), the Dirichlet obstacle being kite-shaped. The thickness of the three half-waveguides W^0, W^1 and W^2 are $h^0 = 1$, $h^1 = 1.2$ and $h^2 = 0.9$, respectively. The junction is a disk of radius 0.8, while the three transverse sections Σ^0, Σ^1 and Σ^2 are located at the same distance $R^j = 3$ ($j = 0, 1, 2$) of the center of such disk. The refractive index is $\eta = 1$ in the whole waveguide, while $k = 40$, which implies that the number of propagating modes in each half-waveguide is $P(0) = 13$, $P(1) = 16$ and $P(2) = 12$, respectively. The figure 14 represents the obstacle which is retrieved when the emitters and receivers are located on a single transverse section Σ^j of a single half-waveguide W^j, for $j = 0, 1, 2$. The figure 15 represents the obstacle which is retrieved on the

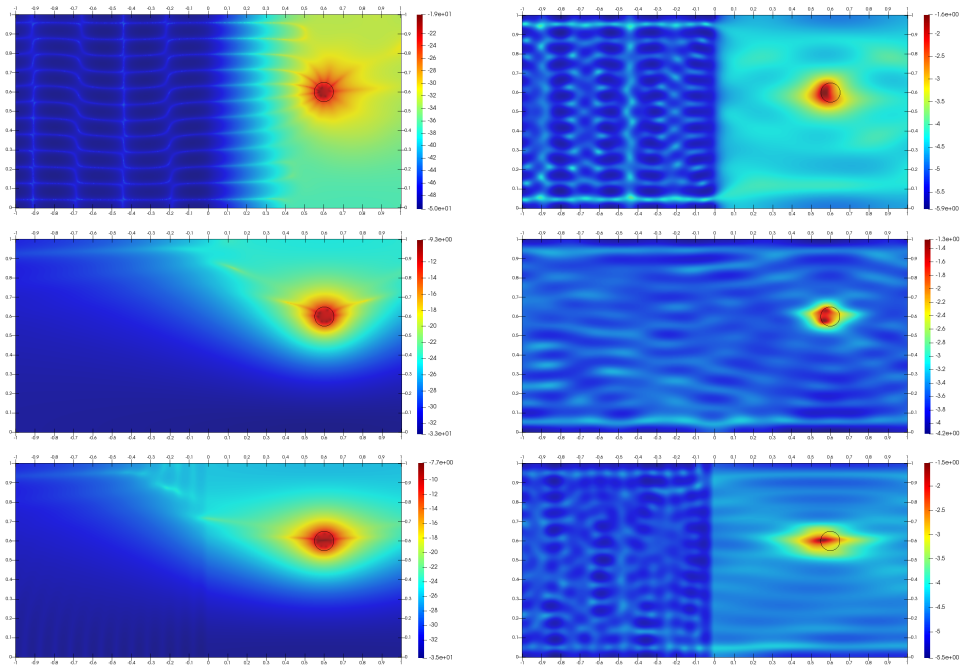

Figure 7: Back-scattering for obstacle 2. Top left: $\kappa = 40$ ($P = 13$) and $\tilde{\kappa} = 20$ ($P = 7$), exact data. Top right: $\kappa = 40$ and $\tilde{\kappa} = 20$, noisy data. Middle left: $\kappa = \tilde{\kappa} = 40$ ($P = \tilde{P} = 13$), exact data. Middle right: $\kappa = \tilde{\kappa} = 40$, noisy data. Bottom left: $\kappa = 40$ ($P = 13$) and $\tilde{\kappa} = 60$ ($\tilde{P} = 20$), exact data. Bottom right: $\kappa = 40$ and $\tilde{\kappa} = 60$, noisy data.

one hand when the emitters and receivers are located on the two transverse sections Σ^0 and Σ^1 of the half-waveguides W^0 and W^1, on the other hand when they are located on all the transverse sections Σ^j of all half-waveguides W^j, for $j = 0, 1, 2$. Unsurprisingly, with or without noise, the larger is the set of data, the better is the identification.

6 Conclusions

The numerical results of the previous section seem to prove that a sampling method such as the Linear Sampling Method can be extended to the case of a junction of several half-waveguides. Some extensions in several directions could be envisioned. Firstly, our method could be extended to elasticity, which is necessary in the context of ultrasonic Non Destructive Testing, as in [9]. Secondly, in the context of NDT, for obvious reasons emitters and receivers cannot be located on transverse sections, but only on the boundary of the waveguide. We can cope with this problem by proceeding as in [7] (acoustics) and in [9] (elasticity), where it is shown that, starting from boundary data, we can come back to data on transverse sections by inverting some emission and reception matrices, the distance between the sensors and their number playing a crucial role in the conditioning of those matrices (see [7]). Lastly, the present article is restricted to the case of Dirichlet obstacles. The generalization

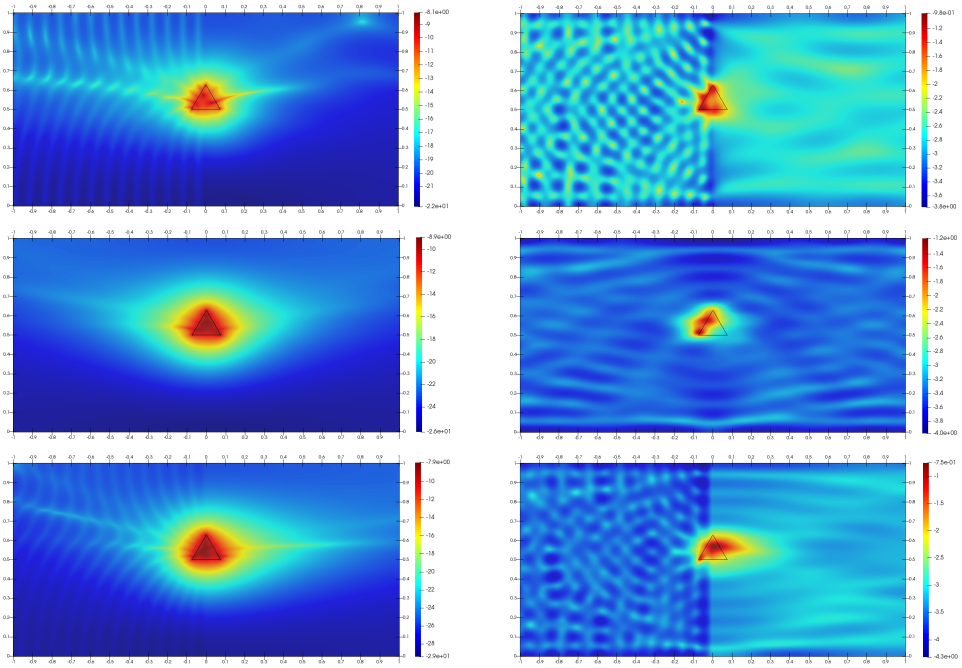

Figure 8: Back-scattering for obstacle 4. Top left: $\kappa = 40$ ($P = 13$) and $\tilde{\kappa} = 20$ ($\tilde{P} = 7$), exact data. Top right: $\kappa = 40$ and $\tilde{\kappa} = 20$, noisy data. Middle left: $\kappa = \tilde{\kappa} = 40$ ($P = \tilde{P} = 13$), exact data. Middle right: $\kappa = \tilde{\kappa} = 40$, noisy data. Bottom left: $\kappa = 40$ ($P = 13$) and $\tilde{\kappa} = 60$ ($\tilde{P} = 20$), exact data. Bottom right: $\kappa = 40$ and $\tilde{\kappa} = 60$, noisy data.

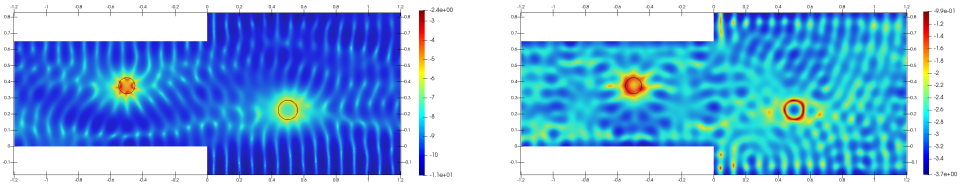

Figure 9: Full-scattering, obstacle 3, $\kappa = \tilde{\kappa} = 40$, $h = 0.65$ ($P = 9$) and $\tilde{h} = 1$ ($\tilde{P} = 13$). Left: exact data. Right: noisy data.

to other types of obstacles is not an issue, for example Neumann obstacles or cracks, following [5] for acoustics and [19] for elasticity.

Acknowledgments

We would like to thank Sonia Fliss for helpful discussions with the authors.

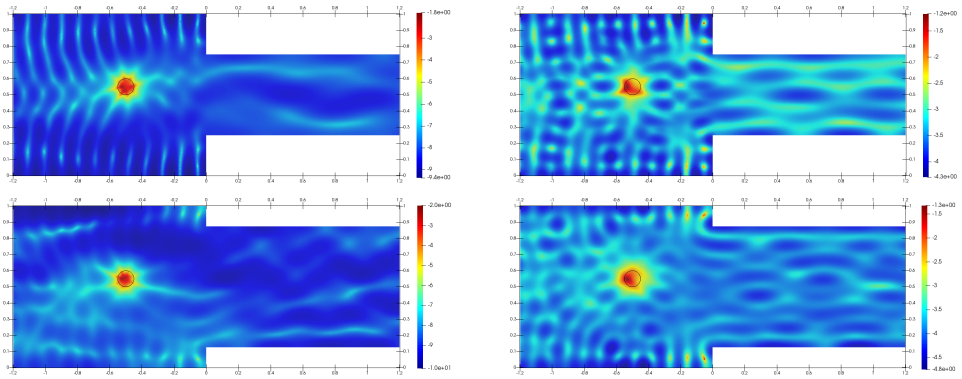

Figure 10: Back-scattering for obstacle 1, $\kappa = \tilde{\kappa} = 30$ and $h > \tilde{h}$. Top left: $h = 1$ ($P = 10$) and $\tilde{h} = 0.5$ ($\tilde{P} = 5$), exact data. Top right: $h = 1$ and $\tilde{h} = 0.5$, noisy data. Bottom left: $h = 1$ ($P = 10$) and $\tilde{h} = 0.75$ ($\tilde{P} = 8$), exact data. Bottom right: $h = 1$ and $\tilde{h} = 0.75$, noisy data.

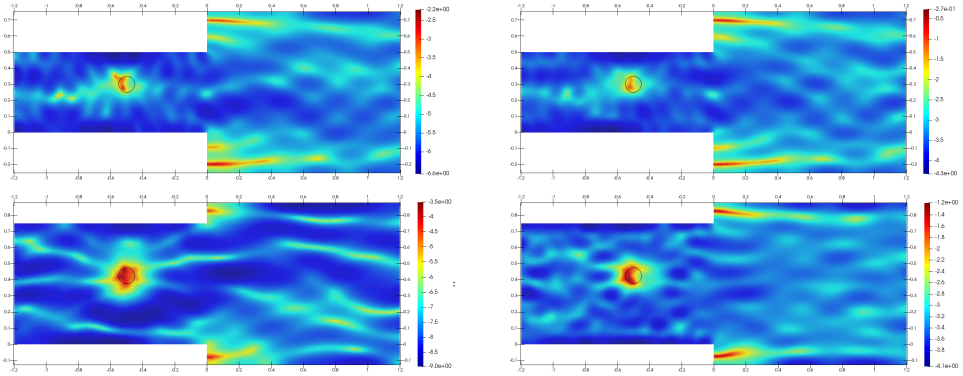

Figure 11: Back-scattering for obstacle 1, $\kappa = \tilde{\kappa} = 30$ and $h < \tilde{h}$. Top left: $h = 0.5$ ($P = 5$) and $\tilde{h} = 1$ ($\tilde{P} = 10$), exact data. Top right: $h = 0.5$ and $\tilde{h} = 1$, noisy data. Bottom left: $h = 0.75$ ($P = 8$) and $\tilde{h} = 1$ ($\tilde{P} = 10$), exact data. Bottom right: $h = 0.75$ and $\tilde{h} = 1$, noisy data.

References

[1] D. Colton and A. Kirsch *A simple method for solving inverse scattering problems in the resonance region*, Inverse Problems, **12,4** (1996), 383–393.

[2] F. Cakoni, D. Colton "Qualitative Methods In Inverse Scattering Theory" Springer-Verlag, Berlin, 2006.

[3] L. Bourgeois and E. Lunéville *The linear sampling method in a waveguide: a modal formulation*, Inverse Problems, **24,1** (2008), 015018, 20 pp.

[4] L. Bourgeois, F. Le Louër and E. Lunéville *On the use of Lamb modes in the linear sampling method for elastic waveguides*, Inverse Problems, **27,5** (2011), 055001, 27 pp.

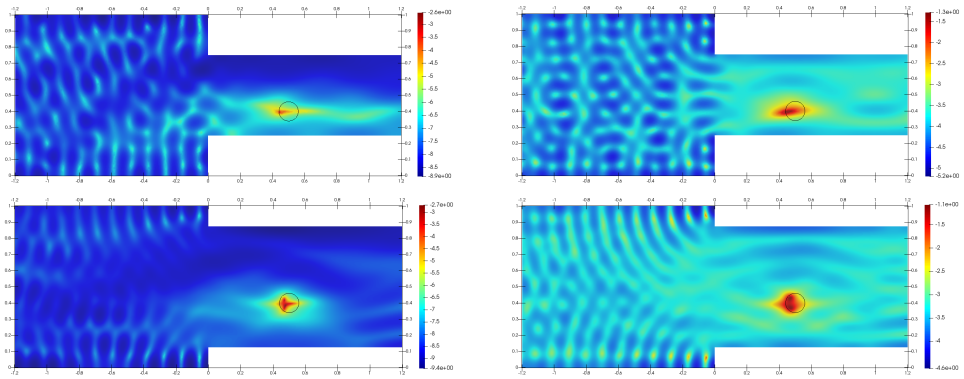

Figure 12: Back-scattering for obstacle 2, $\kappa = \tilde{\kappa} = 30$ and $h > \tilde{h}$. Top left: $h = 1$ ($P = 10$) and $\tilde{h} = 0.5$ ($\tilde{P} = 5$), exact data. Top right: $h = 1$ and $\tilde{h} = 0.5$, noisy data. Bottom left: $h = 1$ ($P = 10$) and $\tilde{h} = 0.75$ ($\tilde{P} = 8$), exact data. Bottom right: $h = 1$ and $\tilde{h} = 0.75$, noisy data.

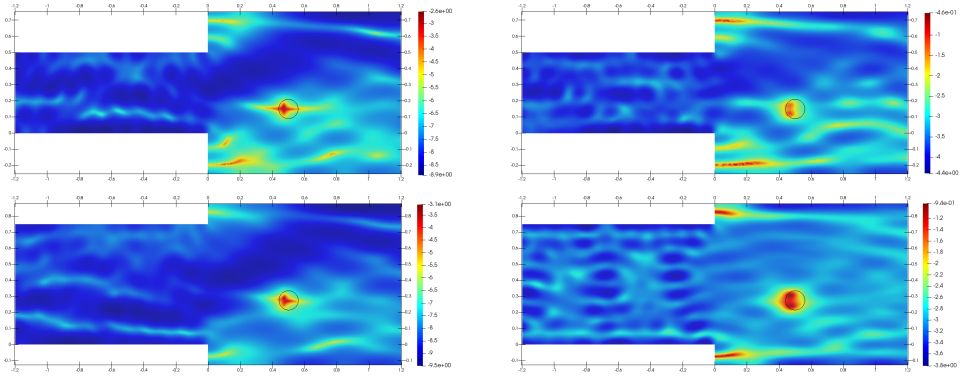

Figure 13: Back-scattering for obstacle 2, $\kappa = \tilde{\kappa} = 30$ and $h < \tilde{h}$. Top left: $h = 0.5$ ($P = 5$) and $\tilde{h} = 1$ ($\tilde{P} = 10$), exact data. Top right: $h = 0.5$ and $\tilde{h} = 1$, noisy data. Bottom left: $h = 0.75$ ($P = 8$) and $\tilde{h} = 1$ ($\tilde{P} = 10$), exact data. Bottom right: $h = 0.75$ and $\tilde{h} = 1$, noisy data.

[5] L. Bourgeois and E. Lunéville *On the use of the linear sampling method to identify cracks in elastic waveguides*, Inverse Problems, **29,2** (2013), 025017, 19 pp.

[6] L. Bourgeois and S. Fliss *On the identification of defects in a periodic waveguide from far field data*, Inverse Problems, **30,9** (2014), 095004, 31 pp.

[7] V. Baronian, L. Bourgeois and A. Recoquillay *Imaging an acoustic waveguide from surface data in the time domain*, Wave Motion, **66** (2016), 68–87.

[8] P. Monk and V. Selgas *An inverse acoustic waveguide problem in the time domain*, Inverse Problems, **32,5** (2016), 055001, 26 pp.

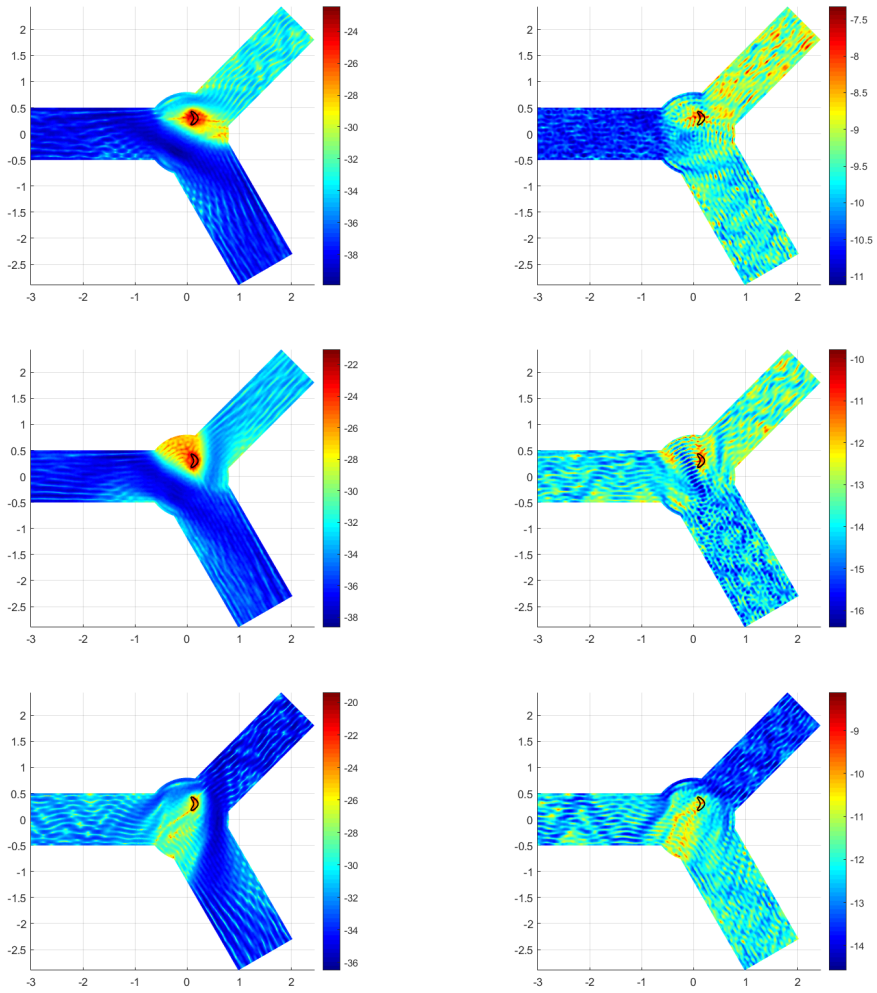

Figure 14: Data on a single half-waveguide. Top left: exact data on section Σ^0. Top right: noisy data on section Σ^0. Middle left: exact data on section Σ^1. Middle right: noisy data on section Σ^1. Bottom left: exact data on section Σ^2. Bottom right: noisy data on section Σ^2.

[9] V. Baronian, L. Bourgeois, B. Chapuis and A. Recoquillay *Linear sampling method applied to non destructive testing of an elastic waveguide: theory, numerics and experiments*, Inverse Problems, **34,7** (2018), 075006, 34 pp.

[10] A. Charalambopoulos, D. Gintides, K. Kiriaki and A. Kirsch *The factorization method for an acoustic wave guide*, in "Mathematical methods in scattering theory and biomedical engineering", World Sci. Publ., Hackensack, NJ, (2006), 120–127.

[11] C. Tsogka, D. A. Mitsoudis and S. Papadimitropoulos *Selective imaging of extended reflectors in two-dimensional waveguides*, SIAM J. Imaging Sci., **6,4**

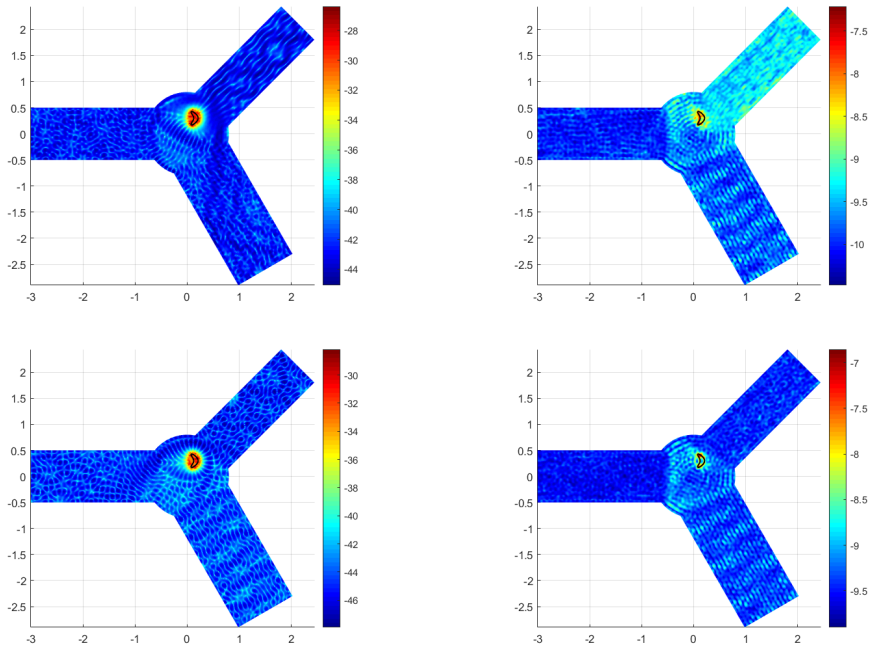

Figure 15: Top: data on two half-waveguides. Left: exact data on sections Σ^0 and Σ^1. Right: noisy data on sections Σ^0 and Σ^1. Bottom: data on three half-waveguides. Left: exact data on sections Σ^0, Σ^1 and Σ^2. Right: noisy data on sections Σ^0, Σ^1 and Σ^2.

(2013), 2714–2739.

[12] C. Tsogka, D. A. Mitsoudis and S. Papadimitropoulos *Partial-aperture array imaging in acoustic waveguides*, Inverse Problems, **32,12** (2016), 125011, 31pp.

[13] C. Tsogka, D. A. Mitsoudis and S. Papadimitropoulos *Imaging extended reflectors in a terminating waveguide*, SIAM J. Imaging Sci., **11,2** (2018), 1680–1716.

[14] L. Borcea, F. Cakoni and S. Meng *A direct approach to imaging in a waveguide with perturbed geometry*, J. Comput. Phys., **392** (2019), 556–577.

[15] L. Borcea and S. Meng *Factorization method versus migration imaging in a waveguide*, Inverse Problems, **35,12** (2019), 0124006, 33 pp.

[16] L. Borcea and S. Meng *Imaging with electromagnetic waves in terminating waveguides*, Inverse Probl. Imaging, **10,4** (2016), 915–941.

[17] P. Monk, V. Selgas and F. Yang *Near-field linear sampling method for an inverse problem in an electromagnetic waveguide*, Inverse Problems, **35,6** (2019), 065001, 27 pp.

[18] A.-S. Bonnet-Bendhia and A. Tillequin *A generalized mode matching method for scattering problems with unbounded obstacles*, Journal of Computational Acoustics, **9,4** (2001), 1611–1631.

[19] L. Bourgeois and E. Lunéville *On the use of sampling methods to identify cracks in acoustic waveguides*, Inverse Problems, **28,10** (2012), 105011, 18 pp.

[20] L. Audibert, A. Girard and H. Haddar *Identifying defects in an unknown background using differential measurements*, Inverse Probl. Imaging, **9,3** (2015), 625–643.

[21] L. Bourgeois and E. Lunéville *The linear sampling method in a waveguide: A formulation based on modes*, Journal of Physics: Conference Series, **135** (2008), 012023.

[22] D. Colton, M. Le Piana and R. Potthast *A simple method using Morozov's discrepancy principle for solving inverse scattering problems*, Inverse Problems, **13,6** (1997), 1477–1493.

E-mail address: laurent.bourgeois@ensta.fr